

Forschungszentrum Karlsruhe
Technik und Umwelt

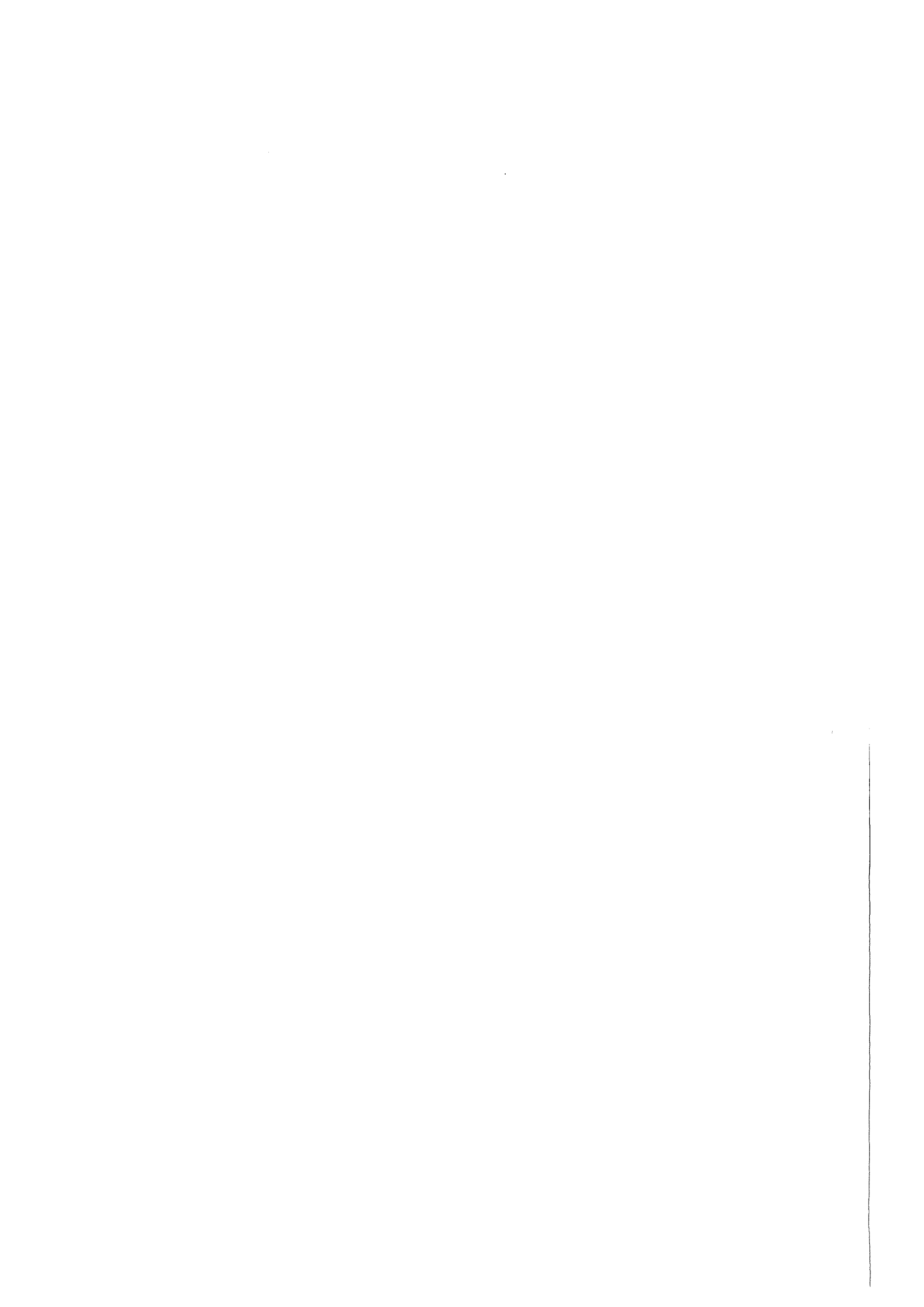
Wissenschaftliche Berichte
FZKA 6192

Electric Fields and ExB Drifts in Hot Plasma Cold Plasma Interactions

I. S. Landman, H. Würz

**Institut für Neutronenphysik und Reaktortechnik
Projekt Kernfusion**

November 1998



Forschungszentrum Karlsruhe

Technik und Umwelt

Wissenschaftliche Berichte

FZKA 6192

Electric fields and ExB drifts in hot plasma cold plasma interactions

I.S. Landman*, H. Würz

Institut für Neutronenphysik und Reaktortechnik

Projekt Kernfusion

* permanent address:

Troitsk Institute for Innovation and Fusion Research
142092 Troitsk, Russia

This work was performed in the frame of ITER; task T226.b and was supported by German WTZ cooperation agreement under RUS-524-96

Forschungszentrum Karlsruhe GmbH, Karlsruhe
1998

Als Manuskript gedruckt
Für diesen Bericht behalten wir uns alle Rechte vor
Forschungszentrum Karlsruhe GmbH
Postfach 3640, 76021 Karlsruhe
Mitglied der Hermann von Helmholtz-Gemeinschaft
Deutscher Forschungszentren (HGF)
ISSN 0947-8620

Abstract

In disruptive hot plasma wall interaction a dense and rather cold plasma shield is formed from evaporated material in front of the target at an early stage of the interaction. Electric potential distributions in the plasma shield hot plasma interaction region and energy deposition profiles were calculated both for perpendicular and for the first time also for inclined impact of the hot magnetized plasma along the guiding magnetic field.

For perpendicular impact, the calculation of the electric potential in the plasma shield is based on the Poisson equation and the condition of zero electric current. The analysis for inclined impact of magnetized hot plasma uses a non-stationary Vlasov Maxwell model, the condition of zero current perpendicular to the target and the existence of an uncompensated current in toroidal direction. In the hot plasma region a significant potential drop occurs resulting in a lateral drift motion (deflection) of the impacting hot plasma. The evolution of an additional magnetic field could result in a self compression of the plasma shield. The dynamics of this self compression and its consequences for the plasma shield stability and for erosion still need more detailed investigations.

Zusammenfassung

Elektrische Felder und ExB Drift bei der Wechselwirkung eines heißen Plasmas mit einem kalten Plasma

Bei der Wechselwirkung eines heißen disruptiven Plasmas mit einem Target bildet verdampfendes Targetmaterial einen dichten, ziemlich kalten Plasmaschild. Elektrische Potentialverteilungen in der Wechselwirkungszone des Plasmaschildes mit dem heißen Plasma und Energiedepositionsverteilungen im Plasmaschild werden für senkrechten und zum ersten Mal auch für geneigten Einfall des heißen magnetisierten Plasmas berechnet.

Für senkrechten Einfall wird die Potentialverteilung im Plasmaschild mittels Poisson Gleichung und der Bedingung eines kompensierten Stromes berechnet. Für die Analyse bei geneigtem Einfall des magnetisierten heißen Plasmas wird ein nicht stationäres Vlasov Maxwell Modell verwendet. Weitere Annahmen sind ein kompensierter Strom senkrecht zum Target und ein Nettostrom in toroidaler Richtung. Im heißen Plasma tritt ein signifikanter Potentialunterschied auf. Dieser verursacht eine laterale Driftbewegung (Ablenkung) des einfallenden heißen Plasmas. Die Evolution eines zusätzlichen Magnetfeldes könnte eine Kompression des Plasmaschildes bewirken. Die Kompressionsdynamik und seine Konsequenz für die Stabilität des Plasmaschildes und damit für die Targeterosion sind noch detaillierter zu untersuchen.

Content

1 INTRODUCTION	1
2 THE PROBLEM	2
2.1 Definition of sheath and pre-sheath	3
2.2 Inclined impact of hot plasma	5
3 MATHEMATICAL DESCRIPTION FOR PERPENDICULAR IMPACT	7
4 SOLUTION FOR PERPENDICULAR IMPACT	12
4.1 The collisionless infinity	12
4.2 Physical parameters and solution of equations	13
4.3 Energy deposition into the plasma shield	16
4.4 The Bohm criteria	17
5 INCLINED IMPACT OF HOT PLASMA	18
5.1 Collisionless region with inclined impact	18
5.2 Collisional region	22
6 THE MAGNETIC PRE-SHEATH AND THE ELECTROSTATIC SHEATH	29
7 CONCLUSIONS	33
8 ACKNOWLEDGEMENT	34
9 REFERENCES	34

1. INTRODUCTION

Results from numerical modeling of disruptive plasma divertor target interactions^{1,2} for the International Thermonuclear Experimental Reactor (ITER)³ and from disruption simulation experiments⁴ have clearly shown that evaporated divertor material forms a dense rather cold plasma shield which protects the target from further excessive evaporation. For the energy deposition of the hot plasma onto the plasma shield an electric field formed in the cold plasma shield hot plasma interaction region has to be known. The field could also influence the overall shielding efficiency of the plasma shield by $\mathbf{E} \times \mathbf{B}$ drift⁵. Therefore the analysis of electric fields in the interaction region is important in prediction of divertor target erosion.

Due to the high mobility of the hot electrons the electric potential of the cold plasma becomes negative in relation to the hot plasma. The potential adjusts in such a way that the quasineutral densities of ions and electrons are balanced differently in the hot and the cold plasma. This results in formation of a space charge region (sheath)⁶ which shields the hot plasma from the negatively charged cold one. Hot electrons are partially reflected from the sheath. Those who overcome the sheath are efficiently decelerated by electric stopping. Hot ions are accelerated in the sheath before being stopped in the cold plasma by collisions.

Sheath formation between a quasineutral plasma and an absorbing solid wall is well known (see the overviews in Ref. 7-10). In Ref. 7 perpendicular impact is considered, in Ref. 8 inclined impact onto an ion absorbing wall is analyzed including the plasma pre-sheath. In Ref. 9 a comprehensive analyses of the sheath theory is presented. A review of some recent investigations of plasma-wall interaction problems including sheath formation and electric drifts of the Scrape-Off Layer (SOL) plasma for inclined magnetic fields is given in Ref. 10.

A simplified analysis of electrostatic shielding for the interface between two plasmas was reported for perpendicular impact of a hot plasma onto a cold plasma shield¹¹. Recently the results of this analysis were applied to the plasma shield hot plasma interaction¹² with inclined impact of the hot plasma. Only the condition of zero electric current in the direction perpendicular to the target was used. A toroidal current which produces a vortex electric field and which is typical for inclined impact was not taken into account. Therefore the results obtained for the potential electric field and the conclusions on the drift motion of the plasma shield represent only a first step towards this problem.

The analysis of plasma wall interaction includes the dynamics of the plasma shield and the disruptive plasma flow in the SOL. The whole problem can be split into independent sub-tasks. The sub-task of the plasma-plasma electrical interaction namely the analysis of the interface between two half-infinite plasmas is discussed in this article for perpendicular and inclined magnetic fields. The parameters of the cold and hot plasma have to be known. The results of the interface analysis allow to define adequately the boundary conditions (e.g. plasma pressure) for numerical calculations of the plasma shield sub-task at the time when the shield thickness is larger than the thickness of the interface. The calculation of the plasma shield evolution is a numerical task for two-dimensional simulation¹³. The sub-task of the disruptive SOL plasma should include the analysis of the thermal contact between the SOL and the main volume of the hot tokamak plasma, the dynamics of the non-stationary propagation of hot ions towards the target, and the analysis of the weekly collisional hot electron sub-

system in the SOL including evolution of plasma loss hyperbolas in the velocity space like that of mirror traps, the physics of which implies the development of kinetic instabilities. Up to now it is not clear whether the sub-system of electrons in the SOL plasma has to be considered as thermally insulated from the main volume of the tokamak plasma during hard disruption events. This circumstance as well as the necessity to describe both the SOL and the hot plasma pre-sheath dynamics using rather complicated collisionless approach make it impossible to choose definitely such an important parameter as the temperature of the hot electrons T_h impacting the shield. Hence presently as boundary conditions for the solution of the plasma-wall interaction the characteristic parameters of the tokamak central plasma are used. Without adequate SOL model lower electron temperatures can't be used. The interface model as given below doesn't require standard tokamak parameters. The model is valid over a wide range of T_h as long as the cold plasma temperature T_c is much less than T_h ($T_c \ll T_h$). A more correct criterion is given in Sec. 4.2. Thus the model keeps practical sense even for the case with a rather cold SOL plasma with insulation from the main tokamak volume or at relatively large times. A discussion on the time scale is given in Sec. 5.2. The suggested model is mainly analytical. Examples are given for ITER typical hard disruptions.

The electric field distribution is derived from a consistent set of equations for perpendicular and inclined impact of the hot plasma. Up to now for the latter no solution is available in literature, for the first no fully consistent plasma-plasma interface model was reported. The analysis for perpendicular impact uses the Poisson equation for the electrostatic sheath and the condition of quasineutrality in the cold and hot plasma outside of it in order to find the potential electric field for the direction perpendicular to the plate (x-direction in our modeling). For the analysis of inclined impact of hot plasma the distribution of electric charges was calculated using the Vlasov equation for the hot plasma and the hydrodynamic equations for the cold plasma. An important feature of inclined impact of magnetized hot plasma is the existence of an uncompensated electric current in the toroidal (z) direction which can reach values of several tenths of kiloamperes as it is shown in Sec. 5.2. This current generates an additional magnetic and a z-directed (toroidal) vortex electric field. For calculation of these fields the Maxwell equations are solved additionally. Diffusion of the magnetic field into the cold plasma is taken into account. From the calculated potential and vortex electric field the energy deposition of the hot plasma into the cold plasma shield and $\mathbf{E} \times \mathbf{B}$ drift effects in both plasmas are derived.

2. THE PROBLEM

The plasma shield near the interface consists of ionized target material of density n_{ci} and temperature T_c and cold electrons of the same temperature and density $n_{ce} = \bar{Z} n_{ci}$ with \bar{Z} the mean charge of the cold plasma. The free path λ_c of the cold particles is much less than the whole thickness of the interface. Thus the cold plasma is described by the hydrodynamics equations in the frame of the cold ions, implying by this way that their velocity is zero in the interface region. Effective energy transfer by radiation and electron heat conduction establishes a rather constant temperature T_c in the cold plasma pre-sheath², therefore it is assumed that T_c and \bar{Z} are constant.

The hot plasma consists of hot electrons of temperature T_h and density n_{he} and of mono-energetic hydrogen like ions of density n_{hi} and energy $w_{hi} = GT_h$ with $G \sim 1$. Due to its rather high temperature ($T_h \gg T_c$) and low density the hot plasma is considered to be collisionless. The process of hot plasma interaction with the plasma shield is both electrical (for hot electrons) and collisional slowing down of the hot particles in the plasma shield. The stopping length of the hot ions λ_{hi} is much smaller than that of the hot electrons λ_{he} which can penetrate into the main volume of the shielding layer. Their stopping length is assumed to be much less than the thickness L of the whole plasma shield.

Density profiles schematically are shown in Fig. 1 for the plasma shield region ($x < 1$) and the hot plasma region $x > 1$ with x the spatial coordinate directed from the target to the core (poloidal direction). The plasma shield region is plotted in units of λ_{he} , the hot plasma region in units of $10 r_D$ with $r_D = (T_h/4\pi e^2 n_{hi}^\infty)^{1/2}$ the Debye radius which describes the characteristic thickness of the sheath. Below such abbreviations of the designation will be used without explanation: $n_{hi}^\infty = n_{hi}(\infty)$, $\varphi_L = \varphi(L)$ etc. The sheath is located at $x = L$. It will be called electrostatic sheath for better distinction against the different pre-sheaths which will be introduced below. It is valid $r_D \ll \lambda_{ce}$ and $r_D \ll \lambda_{ci}$. There are no target material ions far away from the target, $n_{ci}(x)$ vanishes at $x \rightarrow \infty$.

The increase in the density n_{hi} of the hot ions (see Fig. 1) indicates the hot ion stopping region, the density decrease across the sheath their acceleration in the sheath potential. From ITER disruptive plasma-wall calculations^{2,4,14} for the low \bar{Z} targets graphite and beryllium two regions of cold plasma parameters in the shielding layer are obtained. The bulk plasma near the solid target with plasma temperatures of 3-5 eV (here the condition of local thermodynamic equilibrium - LTE is valid, $\bar{Z} \sim 3$) and the plasma corona with temperatures of about 10 eV, ($\bar{Z} = 6$) at larger distances from the target¹⁵. The density values as given in Fig.1 are valid for the corona of the plasma shield. For the bulk plasma the ratio n_{ci}/n_{hi} has to be increased by 3 orders of magnitude.

2.1. Definition of sheath and pre-sheaths

In the sheath a significant part of the hot electrons is reflected collisionless back to the core as is indicated in Fig. 2 for perpendicular impact of the hot plasma onto the cold plasma shield. Fig. 2 shows schematically the potential distribution $\varphi(x)$ in the sheath and the cold plasma. The units of x are the same as in Fig. 1. For the potential distribution $\varphi(x)$ it is assumed $\varphi = 0$ at $x = \infty$ and negative at $x < \infty$. Fig. 2 shows also schematically the particle fluxes. The hot electrons with energies below $e\varphi_\infty$ with φ_∞ the total potential barrier, which are able to overcome the sheath continue to lose their energy in the negative electric potential (electric stopping) and by collisional slowing down in the plasma shield. In a 1 dim model these electrons have no chance to be reflected because their kinetic energy finally approaches the cold plasma temperature T_c and then they join the sub-system of the collisional cold electrons.

In accordance with the guidelines described in Ref. 8 the interface between two different plasmas with $T_c \ll T_h$ is divided into several sub- and pre-sheaths as is shown schematically in Fig. 3 for inclined impact of the hot plasma with inclination angle α . Indicated are also their characteristic sizes. The rather narrow region close to the target (designated with the number 1 in Fig. 3) where due to permanent evaporation the plasma is colder and denser than in the main volume (no.2) is not considered here.

Common to perpendicular and inclined impact are the hot electron collisional (no.3) and electric stopping (no.4) pre-sheaths, the cold plasma pre-sheath (no.5), the electrostatic sheath (no.7) and the hot plasma pre-sheath (no.10). For inclined impact there are added two magnetic pre-sheaths (no.6 and no.8) and an electric drift region (no.9). Because of the rather small density of the hot ions in comparison with the cold ones the ion magnetic pre-sheath in the cold plasma (no.6) is neglected. The meaning of these pre-sheaths is the following:

- the hot electron collisional stopping pre-sheath (no.3) corresponds to the collisional stopping of the hot electrons in the cold plasma
- the hot electron electric stopping pre-sheath (no.4) corresponds to the electric stopping along the guiding magnetic field. The electric barrier of this pre-sheath stops the main part of the hot electrons.
- the cold plasma pre-sheath (no.5) accelerates cold electrons up to their sound velocity at the entrance to the electrostatic sheath. It has the dimension of the order of the free path of the cold electrons λ_{ce} .
- the two magnetic pre-sheaths (no.6 and no.8) have the dimension of the order of the hot ion Larmor radius r_{hi} . The significant potential drop in the electrostatic sheath causes a perturbation of the hot ion gyration trajectories in the vicinity of the sheath, resulting in a change of potential.
- the electrostatic sheath (no.7) the classical sheath.
- the electric drift region (no.9), which is assumed to have the same size l in the x -direction as the plasma shield has in lateral direction, considered as a part of the hot plasma pre-sheath and described in details in Sec. 5.2, provides lateral drift of hot plasma and contains external part of additional magnetic field of the toroidal current as it was mentioned in the Introduction.
- the hot plasma pre-sheath (no.10) is formed by Coulomb collisions of the hot plasma ions. It has the dimension of the order of λ_{hi} and provides acceleration of the hot ions up to their thermal velocity at the entrance to the sheath.

For a tokamak the characteristic length L_s of the disruptive SOL plasma along magnetic field lines is much smaller than λ_{hi} (e.g. in ITER L_s is about $3 \cdot 10^4$ cm and λ_{hi} about 10^7 cm at $T_h = 10$ keV). Therefore the physics of hot ion pre-acceleration should include some other mechanisms providing necessary acceleration, e.g. by geometry (magnetic Laval nozzle) or by turbulent processes switching on collective collisional mechanisms¹⁰. Additional acceleration mechanisms which should be important at relatively short disruption times are due to the non-stationary behavior of the hot ion density n_{hi} at the disruption. For example, for a disruption time $\tau_d = 10^{-4}$ s the ions travel the distance $l_i = v_{Ti} \tau_d = 10^4$ cm with $v_{Ti} = 10^8$ cm/s the ions thermal velocity. For $l_i < L_s$, the hot plasma density drops significantly in the SOL from some maximal value $n_{max}(t)$ at the center of the unstable magneto hydrodynamic (MHD) mode toward the target along the magnetic field line. In the SOL plasma the quasineutrality $n_{he} = n_{hi}$ and the Boltzmann electron density distribution are valid. An electric potential exists, its value is estimated on the base of the equality $n_{hi} = n_{max} \exp(e\phi/T_h)$ with zero electric potential ϕ at $n_{he} = n_{max}$. The potential drop $\phi = (T_k/e) \ln(n_{hi}/n_{max})$ causes pre-acceleration of the hot ions, thermal insulation of hot electrons and additionally enlarges the energy of cold electrons in the SOL after their acceleration in the sheath.

However, as it was mentioned in the Introduction, an adequate hot plasma pre-sheath theory presently is not available. For this reason a simplified approach assumes that the hot ions are mono-energetic. For inclined impact a constant pitch angle is used.

2.2. Inclined impact of hot plasma

The situation for inclined impact schematically is shown in Figs. 4 and 5 with the x-axis defined as previously perpendicular to the target and translation symmetry along the z-axis. The x-axis corresponds to the poloidal direction, the y-axis to the radial direction (along the plate surface) perpendicular to the plane and the z-axis to the toroidal direction. The guiding magnetic field \mathbf{B}_0 with $\mathbf{B}_0 = (B_x, 0, B_z)$ is in the xz-plane. The inclination angle α is defined as

$$\alpha = \arctan(B_x/B_z). \quad (1)$$

It is assumed $\alpha \ll 1$.

An essential feature of the model as shown in Figs. 4 and 5 is the existence of an uncompensated toroidal current $-ej_e$ in the plasma shield. This current may arise because there is no electric charge accumulation in the toroidal direction. The situation with not fully compensated current realizes if cold electrons have some chance to cross magnetic field lines (otherwise the compensation of the z-component follows immediately from the compensation of the x-component). A cold plasma electron after undergoing a Coulomb collision jumps from a magnetic line to another one for the distance of electron Larmor radius. Therefore collisions with ions provide the possibility to get net current. The cold electrons of the plasma shield only compensate the x-component of the electric current of the hot electrons. As schematically indicated in Fig. 5 a compensating current $-eI_0$ is assumed to flow inside of the structure. In the model used this current flows at the distance D from the divertor.

In the transverse direction (y-direction) it is assumed $\partial/\partial y = 0$. The plasma shield is limited in size. Thus the current in this direction is zero for cold and hot electrons separately. The net electron flux \mathbf{j}_e is given as

$$\mathbf{j}_e = \mathbf{j}_{he} - \mathbf{j}_{ce} \quad (2)$$

with \mathbf{j}_{he} and \mathbf{j}_{ce} the hot and cold electron fluxes. Outside of the collisional region the electric current is assumed to be zero. The ion current and external current loops initiated in the core region of the hot plasma are neglected. The z-component of the flux \mathbf{j}_e according to Maxwells equation $\text{rot}\mathbf{B} = -(4\pi/c)\mathbf{j}_e$ with $\partial/\partial y = \partial/\partial z = 0$ produces a y-component of the magnetic field B_y . The equation is given as

$$\frac{\partial B_y}{\partial x} = -\frac{4\pi}{c} ej_e. \quad (3)$$

The arising B_y generates a vortex z-component of the electric field E_z . According to another Maxwells equation $\text{rot}\mathbf{E} = -(1/c)\partial\mathbf{B}/\partial t$ the equation for E_z is given as

$$\frac{\partial B_y}{\partial t} = c \frac{\partial E_z}{\partial x} \quad (4)$$

E_z influences the stopping of hot electrons in the plasma shield. \mathbf{B}_0 is constant because there exists only a z-component of the current. The assumption $\partial/\partial y = 0$ was introduced to simplify the problem removing those features which are not principally changing the main results.

A simple argumentation for the existence of the net current is the following: assuming $\mathbf{j}_e = 0$ then the flux of cold electrons has to compensate the flux of the incoming hot electrons. Due to Ohms law the cold electron current in toroidal geometry produces both a potential $\mathbf{E}_p = (E_x, E_y, 0)$ and a vortex electric field $\mathbf{E}_v = (0, 0, E_z)$. The vortex electric field has closed field lines and generates the magnetic field B_y , which can be created only with $\mathbf{j}_e \neq 0$.

The cold plasma in the collisional region¹⁶ obeys the usual hydrodynamics equations¹⁷ which are applied below in the simplest way in order to arrive at a simple solution. From Ohms law given as

$$\mathbf{E} = -e\mathbf{j}_{ce}/\sigma + [\mathbf{B}\mathbf{j}_{ce}]/cn_{ce}$$

with $\sigma = e^2 n_{ce} \tau_{ce} / m_e$ the electric conductivity, τ_{ce} the momentum relaxation time in the collisions of cold electrons with ions and from Eq. (2) it is clearly seen that the assumption $\mathbf{j}_e = 0$ and the motion of hot electrons along field lines result in the electric field directed along the magnetic field thus formally confirming the simple argumentation. Hence for inclined impact the self consistent non stationary process of formation of electric and magnetic fields has to be included. The full self-consistent model for inclined impact is presented in Sec. 5.

The collisionless ensembles of hot ions and electrons (including cold electrons at $x > L$) gyrating in presence of magnetic and electric fields are described with the Vlasov kinetic equation which allows to calculate adequately the densities and fluxes. The electric and magnetic field is expressed with the help of the electric potential ϕ and the magnetic potential \mathbf{A} according to:

$$\mathbf{E} = -\nabla\phi - (1/c)\partial\mathbf{A}/\partial t, \quad \mathbf{B} = \nabla \times \mathbf{A}. \quad (5)$$

In contrast to the notation for perpendicular impact the electric potential was re-designated ($\varphi \rightarrow \phi$). The reason of this will be clarified below. It is reasonable also to introduce the new coordinates (X, Z) as shown in Fig.4: X- and Z-axes are directed perpendicular and along \mathbf{B}_0 . These new axes are obtained as a result of rotation of the x- and z-axes around the y-axis by the angle α . For the problem described just above it is

$$\phi = \phi(t, \mathbf{x}), \quad \mathbf{A} = (0, B_0 X, A_z(t, \mathbf{x})), \quad (6)$$

$$X = x \cos \alpha - z \sin \alpha, \quad Z = x \sin \alpha + z \cos \alpha \quad (7)$$

with \mathbf{A} being independent from y . Hot particles cross the distance λ_{he} for times which are much less than the characteristic time of the disruption, i.e. thus the problem is quasi-stationary. Due to this the time dependence of the electric potential ϕ is neglected. The coordinates L and D indicated in Fig. 4 denote the positions of the electrostatic sheath (L) and of the compensating current inside the structure (D).

3. MATHEMATICAL DESCRIPTION FOR PERPENDICULAR IMPACT

To tackle this problem the condition of zero electric current is used in the plasma shield and the Poisson equation for $E = -d\phi/dx$ in the sheath. For the cold pre-sheath the quasineutrality condition is used. In terms of particle fluxes the condition of zero current is given as:

$$j_{he} + j_{ce} = j_{hi} \quad (8)$$

The Poisson equation is written as:

$$dE/dx = 4\pi e \delta n \quad \text{with} \quad \delta n = n_{hi} + \bar{Z}n_{ci} - n_{he} - n_{ce} \quad (9)$$

The particle fluxes schematically are shown in Fig. 2. j_{he} is the net flux of the hot electrons, j_{ce} is the flux of the cold electrons that arises in the plasma to compensate j_{he} and the flux of hot ions j_{hi} . As to the flux of cold ions a coordinate system with zero value of this flux is chosen. Fig. 2 also shows the flux j'_{he} of electrons which are reflected at the electrostatic potential.

The boundary condition for Eq. (9) is $E = 0$ at $x = \infty$. From this it follows for the infinity $dE/dx = 0$ and from Eq. (9):

$$n_{he} + n_{ce} = n_{hi} \quad \text{at} \quad x = \infty \quad (10)$$

If the Right Hand Side (RHS) of Eq. (9) could be fully determined and would satisfy cond. (10) then Eq. (9) could be solved. But δn depends on the unknown quantities of ϕ_{∞} and ϕ_L which have to be found from additional boundary conditions. To simplify the problem the smallness of the Debye radius is used. At $r_D \rightarrow 0$ constant potential ϕ at both sides of the sheath is used. Therefore in the approximation $r_D \rightarrow 0$ the two additional boundary conditions:

$$E = 0, \quad x = L, \quad (11)$$

$$n_{he} + n_{ce} = n_{hi} + \bar{Z}n_{ci}, \quad x \leq L. \quad (12)$$

are to be satisfied. The condition (11) has accuracy of characteristic value of E for the cold pre-sheath and is allowed to be used only for the solution of Eq. (9) in the sheath. Condition (12) should be valid everywhere outside of the sheath. L is the coordinate of the interface between the sheath and the cold pre-sheath. The conditions (11) and (12) at $x = L$ are the boundary conditions at '- ∞ ' on the r_D scale (for more details see Ref. 9).

Multiplying Eq. (9) by E and integration over the interval $(x, +\infty)$ results in:

$$\frac{1}{2}E^2 = 4\pi e \int_{\phi}^0 \delta n(\phi') d\phi' \quad (13)$$

with zero charge in the sheath given as:

$$\int_0^{\phi_L} \delta n(\phi) d\phi = 0. \quad (14)$$

The potential profile in the sheath is obtained from the expression:

$$x = \int_{\frac{1}{2}\varphi_L}^{\varphi} \left(8\pi\epsilon \int_{\varphi'}^0 \delta n(\varphi'') d\varphi'' \right)^{-1/2} d\varphi' \quad (15)$$

with $x = 0$ at $\varphi = \varphi_L/2$ in the local frame of the sheath.

The hot electrons are Maxwellian distributed at infinity $x = \infty$. Their density and flux can be calculated for arbitrary x , because due to their uncollisionality they keep the Boltzmann distribution at any cross-section:

$$n_{he} = \exp(e\varphi/T_h) \int_{-\infty}^{v_m} f_M(v) dv, \quad (16)$$

$$j_{he} = \exp(e\varphi/T_h) \int_{-\infty}^{v_m} v f_M(v) dv. \quad (17)$$

The one-dimensional Maxwell distribution function of electron velocity v is given by the expression

$$f_M(v) = n_{he}^{\infty} \left(m_e/2\pi T_h \right)^{1/2} \exp\left(-m_e v^2/2T_h\right). \quad (18)$$

The upper boundary $v_m = \left(2e(\varphi - \varphi_m)/m_e \right)^{1/2}$ of the integration region in Eqs. (16) and (17) is established by the fact that there are no hot electrons coming back from the slowing down region at $x < L$: those electrons would have kinetic energies exceeding the corresponding potential difference: $m_e v^2/2 > e(\varphi(x) - \varphi_m)$. For $\varphi \geq \varphi_L$ it is used $\varphi_m = \varphi_L$. For the region $\varphi_{\infty} \leq \varphi \leq \varphi_L$ it is valid $v_m = 0$, i.e. thus it is assumed that at $T_c \ll T_h$ hot electrons are captured by the cold plasma at the moment of their stopping. Calculating the integrals in Eqs. (16) and (17) yields:

$$n_{he}(x) = \theta n_{he}^{\infty} \exp(e\varphi/T_h) k\left(\frac{e(\varphi - \varphi_L)}{T_h}\right), \quad k(t) = 1 - \frac{1}{2} \operatorname{erfc} \sqrt{\max(0, t)}, \quad (19)$$

$$j_{he} = -\left(\theta/2\sqrt{\pi}\right) v_{The} n_{he}^{\infty} \exp\left(\frac{e}{T_h} \min(\varphi_L, \varphi)\right) \quad (20)$$

with $v_{The} = \sqrt{2T_h/m_e}$ the thermal velocity of the hot electrons. The complementary error function is defined as

$$\operatorname{erfc}(z) = \left(2/\pi^{1/2} \right) \int_z^{+\infty} \exp(-t^2) dt$$

($\operatorname{erfc}(0) = 1$, $\operatorname{erfc}(\infty) = 0$, if $z \gg 1$ then $\operatorname{erfc}(z) \approx e^{-z^2}/\sqrt{\pi z}$). The factor θ takes into account the attenuation of the hot electron flux in the cold plasma due to Coulomb collisions. A rigorous approach for the consistent calculation of Coulomb scattering and slowing down together with electrical stopping would be a rather complicated task which will not be carried out here. Instead of this and for the sake of simplicity the Coulomb attenuation is qualitatively taken into account by the exponential factor θ given as:

$$\theta = \exp\left(\min(0, (x - L)/\lambda_{he})\right). \quad (21)$$

The hot ions are assumed to be mono-energetic having velocity v_{hi}^∞ and density n_{hi}^∞ at infinity. Due to acceleration in the electric field hot ions increase their velocity v_{hi} in the region of the electric potential outside of the slowing down region thus reducing their density as it follows from the flux conservation equation:

$$j_{hi} = n_{hi}(x)v_{hi}(x) = n_{hi}^\infty v_{hi}^\infty. \quad (22)$$

From the energy conservation equation for hot ions it follows:

$$\frac{1}{2} m_i v_{hi}^2 + e\phi = w_{hi}^\infty \quad (23)$$

with m_i the mass of a hot ion and $w_{hi}^\infty = \frac{1}{2} m_i (v_{hi}^\infty)^2$. Calculating $v_{hi}(x)$ from Eq. (23):

$$v_{hi} = v_{hi}^\infty \left(1 - e\phi/w_{hi}^\infty\right)^{1/2}, \quad (24)$$

the density of hot ions is obtained from Eq. (22) and Eq. (24):

$$n_{hi} = n_{hi}^\infty \left(1 - e\phi/w_{hi}^\infty\right)^{-1/2}. \quad (25)$$

The flux of cold electrons both in the collisional and the collisionless region is defined as

$$j_{ce} = n_{ce} v_{ce} \quad (26)$$

with v_{ce} the velocity of the cold electrons. Due to the presence of an electric field in the collisional region the cold electrons move from there to the edge of the shielding layer where the rate of collisions with cold ions decreases but meanwhile the electric field accelerates them. Upon reaching the edge the electrons lose the balance of electric and friction forces. After this they are accelerated and collisionless move to infinity. To describe their behavior the usual hydrodynamic motion equation¹⁷ is used:

$$m_e v_{ce} dv_{ce}/dx = -\left(T_c/n_{ce}\right) dn_{ce}/dx - eE - m_e v_{ce}/\tau_{ce} \quad (27)$$

with $\tau_{ce} = \lambda_{ce}/v_{Tce}$, $v_{Tce} = (2T_c/m_e)^{1/2}$ the thermal velocity of cold electrons. Their free path is given according to expression

$$\lambda_{ce} = \left(3/2\pi\lambda_q\right) T_c^2 / e^4 \bar{Z}^2 n_{ci} \quad (28)$$

with $\lambda_q \sim 10$ the value of the Coulomb logarithm which is assumed to be constant.

The loss of balance corresponds to the region where in Eq. (27) the values of the terms inertial $m_e v_{ce} dv_{ce}/dx$ and pressure gradient $(T_c/n_{ce}) dn_{ce}/dx$ equal the values of both other terms. The equality of the electrical and the friction term in the collisional region expresses the momentum balance and is Ohms law

$$-e j_{ce} = \sigma E . \quad (29)$$

In the collisionless region friction and cold electron pressure gradient and for simplicity the thermal distribution of cold electrons are neglected. Hence the inertial term is equal to $-eE$, i.e. cold electrons obey the energy conservation law:

$$\frac{1}{2} m_e v_{ce}^2 - e\phi = w_{ce}^\infty \quad (30)$$

with $w_{ce}^\infty = \frac{1}{2} m_e (v_{ce}^\infty)^2$. Due to Eq. (26) and Eq. (30) the density and velocity of the cold electrons in the collisionless region are obtained as:

$$v_{ce} = v_{ce}^\infty \left(1 + e\phi/w_{ce}^\infty\right)^{1/2}, \quad (31)$$

$$n_{ce} = n_{ce}^\infty \left(1 + e\phi/w_{ce}^\infty\right)^{-1/2}. \quad (32)$$

The density distribution $n_{ci}(x)$ of the cold ions is a solution of some general hydrodynamic problem for the target material plasma expansion. This is calculated outside of the presented work². Thus in the shielding layer $n_{ci}(x)$ is considered to be a given function of x . As was mentioned above the velocity of the cold ions is assumed to be zero, i.e. their flux is zero, too. Due to small velocities of the cold ions in comparison with electrons and hot ions the consideration for the cold ion flux can be neglected. The structure of the electric field is determined by the relative position of electrons to ions. Owing to their large velocities the fast particles are able to adjust themselves to the current distribution of the cold ions immediately. This quasi-stationary change of the electric field follows from the relatively slow expansion of the shielding layer. As it was mentioned above the coordinate system of the cold plasma edge is considered as a frame of the problem and the problem is analyzed mathematically for a relatively small depth of electrical pre-sheath into the shielding layer in comparison with the layer thickness. The inertial term in the hydrodynamics motion equation vanishes automatically in the chosen frame near the boundary of the whole MHD problem for the plasma shield. Therefore in the collisional region near the edge $x = L$ of the sheath it is still allowed to consider cold ions as being in rest and stationary. They are described by the following equations:

$$-(T_c/n_{ci}) dn_{ci}/dx + \bar{Z}eE + F = 0, \quad F = m_e n_{ce} v_{ce} / (n_{ci} \tau_{ce}). \quad (33)$$

Here F is the force of friction with the cold electrons. In the region of the cold plasma edge at $L-x \sim r_D$ the main force acting on the cold ions in the sheath becomes the electric field. Collisions can be neglected and the electric field determines the profile of the cold ion density. By this way neglecting F in Eq. (33) the Boltzmann density distribution of cold ions in the sheath is obtained:

$$n_{ci}(\phi) = n_{ci}^L \exp(\bar{Z}e(\phi_L - \phi)/T_c). \quad (34)$$

From Eq. (34) formally follows $n_{ci}(\infty) \neq 0$ but this exponentially small leakage of cold ions to infinity will be always neglected.

It should be noted that in any case the cold ion pressure is confined by some part of the hot plasma momentum but at the cold plasma edge the confinement is realized by the self consistent electric field. In other words the pressure balance at the edge results from the momentum of the hot electrons and the reflection of the cold ions from the sheath and from the reaction force due to acceleration of cold electrons and hot ions in the sheath.

The necessary condition for the existence of the sheath when approaching $r_D \rightarrow 0$ is a singularity of the solution of the quasineutral hydrodynamics problem at $x = L$. i.e. formally it should be $E = \infty$ at $x = L$. There is no confusion with the condition (11) because the point $x = L$ is chosen as that of small gradient for the r_D scale problem and simultaneously as that of large gradient for the λ_{ce} scale problem. The problem is described with the four equations (12), (27), (29), (33) for the four unknown variables n_{ce} , n_{ci} , v_{ce} , E at the given electric potentials φ_∞ and φ_L . Rewriting Eq. (33) yields $(T_c/n_{ci})(dn_{ci}/d\varphi) + \bar{Z}e + F/E = 0$, hence $dn_{ci}/d\varphi = -\bar{Z}en_{ci}/T_c$ for $E = \infty$ at $x = L$. This is consistent with Eq. (34). If $T_c \ll T_h$ then the densities of hot ions and electrons in the collisional region will be small in comparison with those of the cold plasma. Then from the quasineutrality condition (Eq. (12)) it is obtained $n_{ce} \approx \bar{Z}n_{ci}$ at $x \leq L$. With this simplification it is obtained from the three other equations together with Eq. (8) and Eq. (20):

$$\left((\bar{Z} + 1)T_c - m_e \bar{Z}v_{ce}^2 \right) dn_{ci}/d\varphi \approx m_e v_{ce}^2 n_{ci} \bar{Z}e/T_h. \quad (35)$$

The term on the RHS being of small value takes into account the dependence of j_{he} on x at $\varphi < \varphi_L$. Taking into account the reflection of hot electrons from the region of strong electric field near $x = L$ then the RHS is becoming still smaller. Due to the smallness of the RHS and due to the inequality $dn_{ci}/d\varphi \neq 0$ the following value for the velocity $v_{ce}(L)$ is obtained:

$$v_{ce}^L = g v_{Tce} \quad (36)$$

with $g^2 = (\bar{Z} + 1)/2\bar{Z}$. Hence cold electrons enter the sheath with their isothermal sound velocity. At the interface between the cold and the hot plasma it is not necessary to introduce a reversed potential drop of value of T_c to artificially prevent penetration of cold electrons into the sheath as was introduced in Ref. 11. The potential $\varphi(x)$ keeps its monotonic behavior everywhere in the shield.

There are no hot ions in the main volume of the cold plasma. It is penetrated only by hot electrons. The stopping of ions brings momentum flux into the cold plasma. From the pressure balance between the cold plasma and this momentum flux:

$$(\bar{Z} + 1)(n_{ci}^\infty - n_{ci}^L) T_c = (m_i n_{hi} v_{hi}^2)_{x=L} \quad (37)$$

the density of the cold plasma ions in the main volume is obtained according to:

$$n_{ci}^{-\infty} = \left(n_{hi}^{\infty} / (\bar{Z} + 1) \right) \left(2w_{hi}^{\infty} / T_c \right) \left(1 - e\phi_L / w_{hi}^{\infty} \right)^{1/2} + n_{ci}^L. \quad (38)$$

This density is attributed to the parts of the shielding layer which are penetrated by hot electrons. The size of this volume is estimated by the collision length λ_{he} of the hot electrons in the cold plasma. λ_{he} is obtained from Eq. (28) using $n_{ci}^{-\infty}$ and T_h instead of n_{ci} and T_c there, as

$$\lambda_{he} = \lambda_{ce} \left(T_h / T_c \right)^2. \quad (39)$$

4. SOLUTION FOR PERPENDICULAR IMPACT

4.1. "The collisionless infinity"

After the derivation of the full physical description and the mathematical notation the problem is solved at first for $\lambda_{he} \ll L$. The aim is to find finally the fluxes of hot electrons and ions before they are slowed down in the shielding layer as well as the boundary condition for the solution of the hydrodynamics problem for the cold plasma.

Before seeking the solution it is noticed that from cond. (10) and Eq. (19) it follows for q the ratio of hot electron to hot ion density at infinity ($q = n_{he}^{\infty} / n_{hi}^{\infty}$):

$$q = \left(1 - n_{ce}^{\infty} / n_{hi}^{\infty} \right) \left(1 - \frac{1}{2} \operatorname{erfc} \sqrt{u_L} \right)^{-1/2} \quad (40)$$

with $u_L = -e\phi_L / T_h$. The values n_{he}^{∞} and n_{hi}^{∞} need not to be equalized as was done in Ref. 11 where the value of the electrostatic potential in the sheath was calculated as $u_L \approx 1.6 \div 1.7$. The constraint $q = 1$ closes the mathematical description without the necessity to use the emitting properties of the cold substance at its boundary. Using this equalization immediately allows to determine from Eq. (40) the density of electrons at infinity:

$$n_{ce}^{\infty} = \frac{1}{2} n_{hi}^{\infty} \operatorname{erfc} \sqrt{u_L} \quad (41)$$

and therefore the electron emission coefficient at the boundary of the cold substance:

$$\Gamma_e = -j_{ce} / j_{he} = 2\sqrt{\pi} n_{ce}^{\infty} v_{ce}^{\infty} e^{u_L} / v_{Th} n_{he}^{\infty} = 2\sqrt{u_L} \operatorname{erfc} \sqrt{u_L} e^{u_L}. \quad (42)$$

Hence the emission coefficient would be defined only by the dimensionless value u_L of the electrostatic potential: $\Gamma_e \approx 2/\sqrt{\pi}$ while $u_L > 1$. In reality the emission coefficient depends on the parameters of the cold substance. For example, if the substance is cold enough then the emission coefficient tends to zero ($\Gamma_e \rightarrow 0$). It is well known that in this case there exists a definite value of u_L ($u_L \sim 3$ depending on the model). In the real plasma shield $\Gamma_e \neq 0$. If there is no reverse flux of cold electrons to infinity ($n_{ce}^{\infty} = 0$) then it is impossible to satisfy Eq. (40) while equalizing n_{he}^{∞} and n_{hi}^{∞} .

It is not adequate to consider “the collisionless infinity” as true because this “infinity” is not the physical infinity of the whole problem (it is only ‘+∞’ in the r_D -scale). Only if there exists local thermodynamic equilibrium at infinity then it is allowed to equalize the densities as mentioned above. The existence of some additional electrostatic potential between the sheath and the far distant collision area of the hot plasma, i.e. a pre-sheath has to be assumed. This potential also accelerates the ions coming from far away to the region of ‘+∞’ and decreases the density of hot electrons there, thus providing the parameter to disconnect the n_{he}^∞ and n_{hi}^∞ . This pre-acceleration of the Maxwellian ions makes it easier to accept the assumption of considering the hot ions as mono-energetic beam. Additionally collisions which change the distribution of particles can influence the value of q . Therefore the problem of potential calculations can only be solved adequately if an analysis of the pre-sheaths is included.

4.2. Physical parameters and solution of equations

Eq. (8) of zero current at $x < L$ is used to obtain the electrostatic potential in the collisional region where hot ions are absent owing to their stopping close to $x = L$. Using Eqs. (20) and (40) Eq. (29) is transformed into:

$$du/d\xi = K \exp(u_L - u - \xi), \quad u|_{\xi=0} = u_L \quad (43)$$

with $u = -e\phi/T_h$, $\xi = (L-x)/\lambda_{he}$. The spatial coordinate x was transformed to the dimensionless quantity ξ . The same was done with the potential. Due to this procedure it is possible to get the important dimensionless parameter K with

$$K = \exp(-u_L) v_{The} e^2 n_{he}^\infty \lambda_{he} / 2\sqrt{\pi} \sigma T_h. \quad (44)$$

K determines the value of the electrostatic potential for the collisional region. From Eq. (43) the potential in the collisional region where the hot ions are already stopped is obtained as long as $\xi \ll 1$. Due to the rather short distance of the stopping of the hot ions it is possible to neglect the potential difference between the edges of the slowing down interval of the hot ions. Below an estimation of the ratio $\lambda_{hi}/\lambda_{he}$ is given. Hence it is obtained:

$$u = u_L + \ln\left(1 + K\left(1 - e^{-\xi}\right)\right), \quad u_{-\infty} = u_L + \ln(1 + K) \quad (45)$$

($u_{-\infty} = -e\phi_{-\infty}/T_h$). This solution doesn't describe the singularity at $x = L$. This problem is discussed below.

The quasineutrality conditions (10) and (12) after using Eqs. (19), (24), (25), (31), (32), (34), and Eq. (40) and transformation to dimensionless parameters take the form

$$qk_L + q_e = 1, \quad (46)$$

$$\frac{1}{2} q e^{-u_L} + q_e \Omega/y = \left(1 + u_L/G\right)^{-1/2} + q_i \quad (47)$$

with $k_L = k(u_L)$, $q_e = n_{ce}^\infty/n_{hi}^\infty$, $q_i = n_{ci}^L/n_{hi}^\infty$, $y = v_{ce}^L/v_{The}$, $G = w_{hi}^\infty/T_h$, $\Omega = (y^2 + u_L)^{1/2}$ and $k(u)$ as given in Eq. (19). For G it is assumed $G \sim 1$. From the condition of zero current at $x > L$ (Eq. (8)) and using Eq. (20), Eqs. (22), Eq. (26) it is obtained:

$$q_e \Omega = q e^{-u_L} / 2\sqrt{\pi} - \gamma \sqrt{G} \quad (48)$$

with $\gamma = (m_e/m_i)^{1/2}$. For the sake of simplicity small contributions of ions to the current are neglected ($\gamma = 0$). The equation of the momentum balance of the sheath (14) after being transformed in the same manner is given as:

$$2u_L / \left((1 + u_L/G)^{1/2} + 1 \right) + \varepsilon^2 q_i = 2q_e u_L \Omega / (y + \Omega) + q \left(k_L - e^{-u_L} \left(\frac{1}{2} + \sqrt{u_L/\pi} \right) \right) \quad (49)$$

with $\varepsilon = (T_c/T_h)^{1/2} \ll 1$.

Thus there is a closed system of four equations (46) - (49), for the four unknown variables q_i , q_e , q , u_L . The dimensionless velocity y of cold electrons at $x = L$ is obtained from Eq. (36): $y = \varepsilon g$.

To simplify the solution of this system the smallness of ε is used. Due to $y \sim \varepsilon$ the expression $y^2 + u_L$ is replaced by u_L and in Eq. (47) the rather small contributions of hot electrons (the term $\sim q$) and hot ions (the term with G) to the quasineutrality at $x = L$ are neglected. Therefore it is obtained for q_i :

$$q_i = \varepsilon^{-1} q_e \sqrt{u_L} / g. \quad (50)$$

q_e is obtained from Eq. (48). For $\gamma = 0$ it is obtained:

$$q_e = q e^{-u_L} / (2\sqrt{\pi u_L}). \quad (51)$$

q is obtained from Eq. (46) as:

$$q = \left(k_L + e^{-u_L} / 2\sqrt{\pi u_L} \right)^{-1}. \quad (52)$$

Now all values are expressed via u_L . u_L is obtained from Eq. (49). Again neglecting small contributions Eq. (49) is written as:

$$G^{-1} u_L = \left(2u_L \frac{1 + e^{-u_L} / 2\sqrt{\pi u_L} k_L}{1 - e^{-u_L} / 2k_L} \right)^2 - 1. \quad (53)$$

For $u_L \gg 1$ it is obtained from Eq. (53) $u \approx 1/4G$. This result corresponds to $G \ll 1$. If the value of u_L decreases then the RHS of Eq.(53) approaches zero. Hence a solution for u_L exists formally for any positive value of G . For this it must be valid $u_L > u_m$ with u_m given by the condition that the RHS of Eq. (53) is zero at $u_L = u_m$:

$$u_m = \left(1 - e^{-u_m} / 2k(u_m) \right) / \left(1 + e^{-u_m} / 2\sqrt{\pi u_m} k(u_m) \right). \quad (54)$$

This equation was solved iteratively starting with $u_m = 1$ in the RHS. As a result it is obtained $u_L \rightarrow u_m \approx 0.49$ for $G \rightarrow \infty$. Values of u_L for some G values as obtained from Eq. (53) are given in Table 1. Concerning the minimum possible value of G (G_{\min}) see the discussion below on the Bohm criterion.

Now the features of the potential distribution in the collisional region can be described. Substituting all known values into Eq. (44) it is obtained:

$$K = \varepsilon^{-1} (\bar{Z} + 1) q e^{-u_L} / (2\sqrt{\pi} \sqrt{G + u_L}). \quad (55)$$

With ε as small parameter ($K \gg 1$) it is obtained from Eq. (45) $u_\infty \approx -\ln \varepsilon \gg 1$. From this it is concluded that at the depth larger than λ_{he} the change of the electric potential in the collisional region is becoming small. Therefore the influence of the electric field on the stopping of electrons in the main volume can be neglected. But due to the large value of u_∞ the main part of the hot electrons is electrically stopped in the relatively narrow region near the edge of the shielding layer. Then they come back as reverse current of cold electrons depositing their energy by Ohmic heating.

A more adequate description of this electric stopping region needs more details such as consideration of the Knudsen layer between the collisional region and the sheath to take into account escaping of cold run-away electrons from the cold pre-sheath. Additionally reflection of hot electrons from the electrical pre-sheath should be considered. In this case the inclined motion of hot electrons with respect to the guiding magnetic field has to be taken into account. Such a more complicated description is still lacking and could be performed in a next analysis of the interface problem between the cold and the hot plasma.

Now an upper estimation for the ratio of the hot ion stopping length λ_{hi} to the hot electron stopping length λ_{he} is given. The equation of slowing down of hot ions by cold electrons is given as¹⁸:

$$dv_{hi}/dx = -n_{ce}\Gamma_t m_t / m_e v_c^3, \quad v_{hi}|_{x=L} = -v_{hi}^L, \quad (56)$$

with $\Gamma_t = 6T_h^2 / (\lambda_{he} n_{ci} m_t^2)$, m_t the mass of the cold ion, $v_{hi}^L = \gamma v_{The} (G + u_L)^{1/2}$, $v_c \approx v_{Tce} \gamma^{2/3}$. Integrating this equation over the interval $L - \lambda_{hi} < x < L$ yields:

$$v_{hi}^L = 6\bar{Z}\Gamma_h^2 \lambda_{hi} / (\lambda_{he} m_i m_t v_c^3)$$

and then:

$$\xi' < \lambda_{hi} / \lambda_{he} = (2m_t \varepsilon^2 / 3\bar{Z} m_i \gamma) (G + u_L)^{1/2}. \quad (57)$$

Hence the assumption $\lambda_{hi} \ll \lambda_{he}$ is correct only for small ε (practically $\varepsilon < 0.3$).

The behavior of the electrostatic potential in the interval $0 < \xi < \xi'$ with $\xi' = \lambda_{hi} / \lambda_{he}$ can be described by Eq. (45) as long as $\xi > \lambda_{ce}(L) / \lambda_{he} \sim \varepsilon^3$, because the hot ion current is negligibly small and the coefficient of electrical conductivity σ doesn't depend on the density. At $\xi \leq \varepsilon^3$ (i.e. at the distances from the sheath comparable to free

path of cold plasma particles) all terms in Eqs. (27) and (33) are significant. But to account for all of them is not enough for a spatial resolution of the above mentioned potential singularity at the sheath. As it is usual for hydrodynamic problems it is necessary to have in addition some dissipative terms (describing viscosity and/or heat conduction) to get the spatial dependencies near the singularity at $x = L$. It is not necessary to analyze this structure here because the only characteristic value of energy in the region of singularity is T_c , i.e. which adds only a negligibly small correction of the order of T_c/e to the potential $\phi(x)$. The calculated spatial dependence of the dimensionless potential $u(x)$ is shown in Fig. 2.

4.3. Energy deposition into the plasma shield

Finally the energy fluxes $Q_{e0}^{(0)}$ and Q_{eL} of the hot electrons to the main volume and to the electrical pre-sheath and the energy flux Q_i deposited into the cold plasma by the hot ions are calculated without attenuation factor θ . The flux $Q_e^{(0)}$ transported by electrons reaching the points $u \geq u_L$ is given by the integral:

$$Q_e^{(0)}(u) = e^{-u} \int_0^\infty \frac{1}{2} m_e v^2 v f_M(v) dv = n_{hc}^\infty v_{Th} T_h e^{-u} / \sqrt{\pi}. \quad (58)$$

Q_i is given by the expression:

$$Q_i = n_{hi}^\infty v_{hi}^\infty (w_{hi}^\infty - e\phi_L). \quad (59)$$

Expressing Q_{eL} and Q_i in terms of $Q_{e0} = Q_e^{(0)}(u_{-\infty})$ it is obtained:

$$Q_{eL} = Q_{e0} (e^{u_{-\infty} - u_L} - 1) = K Q_{e0}, \quad (60)$$

$$Q_i \approx Q_{e0} (\bar{Z} + 1) \gamma \sqrt{G} / (2\varepsilon). \quad (61)$$

With the factor θ no electrons are reaching the potential region of $u \rightarrow u_{-\infty}$. Therefore Q_{e0} gives an estimation of the net Coulomb stopping contribution. Q_{eL} provides a rather correct value of the net electrical stopping contribution as long as the main part of the electrons is absorbed in the region of size less than λ_{he} . The distribution of the whole hot electron energy deposition in accordance with Eq. (43) is given as:

$$dQ_e/dx = (du/dx) d(\theta Q_e^{(0)})/du.$$

In accordance with Eq. (45) dQ_e/dx is proportional to $((K+1)e^{\xi} - K)^{-2}$. This is shown in Fig. 6. The width of the electrical pre-sheath λ_E can be defined as the distance of half absorption, corresponding to the value of u given as $Q_e(u)/Q_{eL} = 0.5$. Then it follows from Eq. (45) at $K \gg 1$: $\lambda_E \approx \lambda_{he}/K$.

Values for different parameters discussed in this section are given in Table 2 for $G = 1$, $\gamma = 1/70$, $\bar{Z} = 6$, $\varepsilon = 1/10$ to demonstrate their characteristic size. The energy deposition into the main volume is K times smaller than into the electrical pre-sheath.

The energy deposition of ions at $G \sim 1$ is practically of the same order as Q_{eo} (ions are important from the point of the momentum transfer). Fig. 1 rather qualitatively describes the density distributions for the mentioned case. E.g. it shows in addition the peak of the density of the hot ions arising from the stopping of the ion beam. The decrease of the cold ion density in the sheath as shown in Fig. 1 is not so abrupt as it should be in accordance with Eq. (34).

The whole electron energy flux Q_{ew} is obtained by subtracting the flux of cold electrons $Q_{ce} = \frac{1}{2}m_e[n_{ce}(v_{ce})^3]_{x=\infty}$ from $Q_e^{(0)}(u_L)$. From Eqs. (51) and (58) it follows:

$$Q_{ew}(u_L) = Q_e^{(0)}(u_L)\left(1 - \frac{1}{2}u_L\right).$$

Comparing this expression and the heat flux without the sheath $Q_{ew}(0)$ the factor of the electron heat insulation by the sheath is obtained as $\kappa = \exp(-u_L)(1 - u_L/2)$. For example, in accordance with Table 1 this factor for $G = 1$ is obtained as $\kappa = 3.1$.

4.4. The Bohm criterion

The Eqs (18) and (19) for the hot electron distribution function and their density are valid rigorously only if the electric potential depends monotonically on x , otherwise regions in the velocity space v are arising which cannot be accessed by the collisionless hot electrons. Moreover a non-monotonic situation can result in the development of plasma instabilities. Therefore it should be established a criterion for the monotonic behavior of the potential.

Substituting Eqs. (19), (25), (32) and (34) into Eq. (13) and converting to dimensionless variables it is obtained for the potential in the limit $\varepsilon \rightarrow 0$:

$$\begin{aligned} \Phi(u) = \int_0^u \delta n / n_{hi}^\infty du = & 2u / \left(\sqrt{u/G+1} + 1 \right) - 2q_e u \sqrt{u_L} / \left(\sqrt{u_L} + \sqrt{u_L - u} \right) - \\ & - q \left(k_L - e^{-u} k(u_L - u) \right) - q e^{-u_L} / \left(\sqrt{\pi u_L} + \sqrt{\pi(u_L - u)} \right) \end{aligned} \quad (62)$$

with $\Phi \propto (du/dx)^2$. Requiring now a rigorously positive value of Φ for the limit $x \rightarrow \infty$ (at $u \rightarrow 0$) expressed as $\min \Phi > 0$ results in the Bohm criterion. The required condition is a necessary but not a sufficient condition for the monotonic behavior. At $u \rightarrow 0$ Eq. (62) transforms into

$$\Phi(u) \rightarrow \frac{1}{2} u^2 \Phi''(0) = \left(1 - q_e / 2u_L - \frac{1}{2} G^{-1} \right) u^2 / 2, \quad (63)$$

i.e. $\Phi > 0$ while the expression in the brackets is positive. Introducing Eq. (51) and (53) for q_e and u_L results in a lower limit of the hot ion energy G_{min} given as:

$$G > G_{min} = \frac{1}{2} \left(1 - e^{-u_L} / \left(4\sqrt{\pi} u_L^{3/2} \left(k_L + e^{-u_L} / 2\sqrt{\pi u_L} \right) \right) \right)^{-1}. \quad (64)$$

The calculated minimum value of G (G_{min}) with u_L satisfying Eq. (53) is 0.5. According to Table 1 it is seen that all points listed there are satisfying the Bohm criterion.

From Eq. (15) it is obtained:

$$x = r_D \int_u^{u_L/2} (2\Phi(u'))^{-1/2} du' \quad (65)$$

and thus the asymptotic value of u at $x \rightarrow \infty$ is given as:

$$u \propto \exp\left(-\sqrt{\Phi''(0)} x/r_D\right) \quad (66)$$

Hence it follows that when approaching the margin of the stability (i.e. $\Phi'' \rightarrow 0$) the sheath penetrates infinitely into the hot plasma.

5. INCLINED IMPACT OF HOT PLASMA

5.1. Collisionless region with inclined impact

At early times the additional magnetic field B_y (see Eq. (3)) is much less than $|\mathbf{B}_0|$. Therefore the perturbations A_z with $B_y = -\partial A_z/\partial x$ are neglected. But it is to remind that $E_z = -(1/c)\partial A_z/\partial t$ substantially effects the stopping of the hot electrons.

The behavior of collisionless hot particles in non-stationary fields is described by the Hamilton function H^{19} . H is given according to:

$$H(t, x, z, \mathbf{p}) = (1/2m) \left(p_x^2 + (p_y - B_0(e/c)X)^2 + (p_z - (e/c)A_z(t, x))^2 \right) + e\phi(x) \quad (67)$$

with $\mathbf{p} = (p_x, p_y, p_z) = m\mathbf{v} + (e/c)\mathbf{A}$ the canonical momentum, \mathbf{v} the particle velocity. The particles are described with the distribution function $f(t, x, z, \mathbf{p})$. Symmetry along the y -direction is assumed. Symmetry along the z -direction conveniently will be used later. The value of the distribution function is constant along the trajectory of a collisionless particle, i.e. f is the motion integral. Its time derivation along the particle trajectory is zero:

$$\frac{df}{dt} = \frac{\partial f}{\partial t} + \{H, f\} = \frac{\partial f}{\partial t} + \frac{\partial H}{\partial p_x} \frac{\partial f}{\partial x} - \frac{\partial H}{\partial x} \frac{\partial f}{\partial p_x} + \frac{\partial H}{\partial p_z} \frac{\partial f}{\partial z} - \frac{\partial H}{\partial z} \frac{\partial f}{\partial p_z} = 0 \quad (68)$$

with $\{H, f\}$ the Poisson brackets.

Eq. (68) is the Vlasov kinetic equation for the distribution function. From the independence of H from y follows $\{H, p_y\} = 0$. To determine the three component vector \mathbf{p} for each point (x, z) the function f should be expressed via three motion integrals. Their values are to be fixed by the initial conditions of the trajectories, i.e. f should depend on p_y and some two additional motion integrals. From the fact that the time derivation of H along the particle trajectory is equal to its partial derivation the following motion integral is obtained:

$$dH/dt = \partial H/\partial t = -v_z(e/c)\partial A_z/\partial t. \quad (69)$$

Therefore along the trajectory the following expression remains constant:

$$H' = H - e \int_{-\infty}^t E_z v_z dt' \quad (70)$$

i.e. H' is the second integral. As will be shown below the integral in Eq. (70) is mainly a function of x . For $\alpha \ll 1$ a third motion integral can be found. It is the adiabatic invariant. Its value remains constant along the trajectory (small oscillations of the order of α are neglected). The expression for the adiabatic invariant considering H' in the new XZ-frame, neglecting small A_z and assuming Z constant during one gyration cycle is obtained. Hence the canonical momentum $p_{\parallel} = p_x \sin \alpha + p_z \cos \alpha$ corresponding to Z is also constant. Therefore H' can be considered to be the Hamilton function of some one-dimensional system oscillating along the X-axis. Then in accordance with Ref. 19 the adiabatic invariant can be expressed by the integral:

$$I = (\omega/\pi) \int_{X_{\min}}^{X_{\max}} p_X dX \quad (71)$$

with $\omega = eB_0/mc$ the gyration frequency and p_X the canonical momentum corresponding to the X-coordinate. p_X is given according to

$$p_X^2 = 2m(H_{\perp} - e\varphi) - (p_y - m\omega X)^2 \quad (72)$$

$$\text{with } H_{\perp} = H' - p_{\parallel}^2/2m \quad \text{and} \quad \varphi = \phi - \int_{-\infty}^t E_z v_z dt', \quad (73)$$

X_{\min} and X_{\max} are the roots of the equation $p_X = 0$ (stopping points of oscillation along X). In Eq. (73) an 'effective potential' φ is introduced which is assumed to vanish at $x \rightarrow +\infty$. As will be shown below the effective potential in case of inclined magnetic field plays the same role as the electric potential ϕ in case of perpendicular impact. This is the reason for using the same designation φ .

The calculation of the integral in Eq. (71) at $\varphi = 0$ yields $I = H_{\perp}$. The stopping points are

$$X_{\min}, X_{\max} = p_y/m\omega \pm \sqrt{2H_{\perp}/m\omega^2}.$$

From this the value of p_y is determined by the coordinate $X_c = (X_{\min} + X_{\max})/2$ being the transversal projection of the effective center of the particle trajectory ('the leading center'): $p_y = m\omega X_c$ (this is the formal definition of X_c). From the symmetry along the z-direction follows that the distribution function doesn't depend explicitly on p_y : $f = f(H', I)$. Otherwise it would depend on X_c , hence in accordance with Eq. (7) on the z-coordinate of the leading center at fixed x-values.

Density and flux of particles are expressed according to:

$$n = \int f d\mathbf{v}, \quad \mathbf{j} = \int \mathbf{v} f d\mathbf{v}. \quad (74)$$

The distribution function of the Maxwellian hot electrons of temperature T_h normalized to the core electron density n_{he}^{∞} depends explicitly only on H' :

$$f_{\text{he}} = f_{\text{he}}(H') = n_{\text{he}}^{\infty} (m_e/2\pi T_h)^{3/2} \exp(-H'/T_h). \quad (75)$$

Such an expression for f_{he} is valid only for the trajectories of particles coming from the region $x = +\infty$ (including the part of trajectories after possible reflection from the effective potential). The effective potential is assumed to be a monotonically increasing function of x . Then there should exist additional trajectories originating at $x = -\infty$ (in the electrical pre-sheath) but there are no closed ones. If all trajectories would be populated and would have the same Maxwellian distribution function (see Eq. (75)) then Eq. (74) could be integrated over all the trajectories using Eq. (75) for arbitrary velocities resulting in the Boltzmann density distribution: $n_{he} = n_{he}^{\infty} \exp(e\varphi/T_{he})$. Because there is no hot electron reflection from the region $\varphi(x) < \varphi_L$ the trajectories are unpopulated if electrons are coming from the electrical pre-sheath (φ_L is the effective potential at $x = L$). It is not allowed to integrate in Eq. (74) over the velocities belonging to those trajectories.

To determine the empty domain $f_{he} = 0$ of the electron velocity space the adiabatic invariant I as defined in Eq. (71) has to be calculated. This can be done if it is assumed that the electron Larmor radius r_{Lhe} is much less than the minimum characteristic length of the effective potential change given by the Debye radius r_D . That is $r_{he} \ll r_D$ where $r_{he} = v_{The}/\omega_e$, $\omega_e = eB_0/m_e c$. Below this assumption always is used.

Hence the change of potential can be neglected at $X_{min} < X < X_{max}$, and from Eq. (71) it is obtained $I = H_{\perp} + e\varphi$. From this it is seen that the adiabatic invariant is the kinetic energy of the transverse motion $m_e v_{\perp}^2/2$ with $v_{\perp}^2 = v_x^2 + v_y^2$. Therefore the only value that changes in the course of the motion is the velocity component $v_{\parallel} = p_{\parallel}/m_e$ parallel to \mathbf{B}_0 . The energy conservation is given as

$$H' - I = \frac{1}{2} m_e v_{\parallel}^2 - e\varphi = \text{const}. \quad (76)$$

The transverse part of the electron energy remains constant along the trajectory. Therefore integration over v_x and v_y in Eq. (74) can immediately be performed with the Maxwellian function for electrons (see Eq. (75)). By this way the same Eqs. (19) and (20) as for the case with perpendicular impact as functions of the effective potentials φ and φ_L are obtained. The attenuation factor (see Eq. (21)) is changed accounting for the inclination of hot electrons with respect to the x -axis:

$$\theta = \exp\left(\min(0, (x-L)/\lambda_{he} \sin \alpha)\right). \quad (77)$$

The other species of collisionless particles are cold electrons. They are accelerated in the sheath. Their density n_{ce} and flux j_{ce} in Z -direction is calculated also using Eq. (76) but neglecting the relatively small value of the initial kinetic energy of the cold electrons at $\varphi = \varphi_L$. Due to the conservation of the adiabatic invariant it is used $v_{\perp}=0$. The distribution function of the cold electrons is written as

$$f_{ce} = C_e \delta\left(\frac{1}{2} m_e v_{\parallel}^2 - e\varphi + e\varphi_L\right) \delta\left(\frac{1}{2} m_e v_{\perp}^2\right), \quad C_e = \left(m_e^2 n_{ce}^{\infty} / 2\pi\right) (-2e\varphi_L / m_e)^{1/2} \quad (78)$$

with the normalization constant C_e obtained from Eq. (74), and the Dirac δ -function:

$$\delta(\nu) = \begin{cases} 0, & \nu \neq 0; \\ \infty, & \nu = 0 \end{cases}, \quad \int_{-\infty}^{+\infty} \delta(\nu) d\nu = 1.$$

From this the Eqs. (31) and (32) for n_{ce} and $v_{ce} = j_{ce}/n_{ce}$ with $w_{ce}^{\circ} = -e\phi_L$ are obtained.

Eq. (73) is transformed at $v_z < 0$ into:

$$\varphi = \phi(x) + \int_z^{+\infty} E_z(x') dz' \quad (dz' = v_z dt'). \quad (79)$$

Due to the small oscillation amplitude along x the x' -coordinate in E_z is replaced by that of the leading center x_c . As it is belonging to the magnetic field line, it is valid $x_c \cos \alpha - z' \sin \alpha = \text{const}$. From this it is obtained neglecting the difference in x and x_c :

$$\varphi(x) = \phi(x) + \text{ctg} \alpha \int_x^{+\infty} E_z(x_c) dx_c \quad (|dE_z/dx| \ll |E_z|/(X_{\max} - X_{\min})). \quad (80)$$

Eq. (80) is valid if the shift of the x -location of the particle during a gyration cycle is small (i.e. the conservation of H' is valid with a small oscillation). It will be shown that even for hot ions Eq. (80) is valid also in the rather narrow vicinity of the sheath $x \sim L \pm r_{hi}$ (i.e. in the ion pre-sheath, where $r_{hi} = v_{hi}^{\circ}/\omega_i$, $\omega_i = eB_0/m_i c$). The analysis of the ion pre-sheath is completed in Sec. 4.

Now the collisionless transition region at $x > L + r_{hi}$ defined as the electric drift region in Sec. 2.1 will be analyzed keeping in mind the connection between the core and the ion pre-sheath. The incoming flux of hot ions is assumed to have the density n_{hi}° at $x = +\infty$, definite ion energy H_0 and the pitch-angle defined as the angle θ_0 between the direction of \mathbf{B}_0 and the ion velocity vector \mathbf{v} . For ions $I = I_0 = H_0 \sin^2 \theta_0$, $m = m_i$. As distribution function it is obtained:

$$f_{hi} = C_i \delta(H' - H_0) \delta(I - I_0), \quad \text{with} \quad C_i = n_{hi}^{\circ} \sqrt{2m_i H_0} m_i \cos \theta_0 / 2\pi \quad (81)$$

For $I = H_L - e\varphi$ Eq. (81) for small Larmor radius transforms into:

$$f_{hi} = C_i \delta\left(\frac{1}{2} m_i v_{\parallel}^2 - H_0 \cos^2 \theta_0 + e\varphi\right) \delta\left(\frac{1}{2} m_i v_{\perp}^2 - H_0 \sin^2 \theta_0\right). \quad (82)$$

After substitution of Eq. (82) into Eq. (74) the Eqs. (25) and (26) are obtained for the hot ion density n_{hi} and the velocity $v_{hi} = j_{hi}/n_{hi}$ parallel to the Z -axis with φ the effective potential and $w_{hi}^{\circ} = H_0 \cos^2 \theta_0$.

As it was mentioned in Sec. 2.2 it must be valid $j_c = 0$ at $x > L$, i.e. in accordance with Eq. (3) there exists a spatially constant magnetic field $B_y = B_y^L$. The x dependence of B_y is shown schematically in Fig. 7. In reality owing to the limited size of the vapor shield in y -direction such a magnetic field should gradually vanish in the electric drift region far away from the current conductor location in the vapor shield. For the sake of simplicity it is assumed here that the field is vanishing abruptly due to some artificial z -directed electric current $-eI_0$ which compensates the current of the shield and which is located at $x = D$ (see Fig. 5). The distance $l = D - L$ is assumed to be of the order of the vapor size in y -direction and defines the size of the electric drift region. It is assumed $l \gg r_{hi}$. The implication of an abrupt boundary necessarily equates the 'abstract' point $x = +\infty$ and the definite point $x = D$. It is assumed also that the hot core is situated at $X \geq D$. From Eq. (4) the vortex electric field at $L \leq x \leq D$ can be obtained:

$$E_z = -(D - x) \dot{B}_y^L / c. \quad (83)$$

In Eq. (83) the boundary condition $E_z(D) = 0$ was used to satisfy the requirement that the electric field vanishes at infinity. The dot above B_y designates the time derivation d/dt . Using $\phi(D) = 0$, $\phi(0) = 0$ then from Eq. (80) and (83) it is obtained:

$$\phi(x) = \phi(0) - (ctg\alpha/2c)(D - x)^2 \dot{B}_y^L. \quad (84)$$

To determine ϕ in the electric drift region the quasineutrality equation $n_{hi} = n_{he} + n_{ce}$ is used. Substituting Eqs. (19), (25) and (32) into this equation it is recognized that the solution ϕ doesn't depend on x , i.e. in the electric drift region it is valid $\phi = 0$. Then the behavior of the electric potential ϕ immediately follows from Eq. (84): it compensates the vortex term. The hot plasma propagates freely up to the ion pre-sheath but an electric field $E_x = -\partial\phi/\partial x$ arises in the electric drift region. This field causes an electric drift of the hot plasma along the y -direction (in lateral direction) being the reason of the region's name. The drift velocity v_d is given as $v_d = cE_x/B_0$. The calculation of E_x requires the analysis of the collisional region.

5.2. Collisional region

In the collisional region that includes the cold and electrical pre-sheaths it is convenient to consider cold and hot electrons as one system. The unknown value of ϕ_L is obtained in Sec. 6. The distribution function f_e of all electrons belonging to this system consists of two parts: full Maxwell distribution of temperature T_c and density $n_{ce} \approx \bar{Z}n_{ci}$ as well as half-Maxwell distribution of temperature T_h and density n_{he} with negative component of electron velocity parallel to \mathbf{B}_0 . The quasi-stationary momentum equation for this electron system is given as¹⁷:

$$\frac{\partial}{\partial x} \left(m_e n_e \langle v_x v_\beta \rangle \right) + en_e E_\beta + \frac{e}{c} [\mathbf{j}_e \mathbf{B}]_\beta = R_\beta \quad (85)$$

with $\beta = x, y, z$, $\langle v_x v_\beta \rangle = (1/n_e) \int v_x (v_\beta - v_{e\beta}) f_e dv$ and $R_\beta = -m_e n_{ce} v_{ce\beta} / \tau_{ce}$. R_β is the β -component of the friction force that describes mainly collisions of the cold electron subsystem with the cold vapor ions of the plasma shield. The mean velocity of electron system \mathbf{v}_e is given as $\mathbf{v}_e = \mathbf{j}_e / n_e$, the whole electron density n_e is $n_e \approx n_{ce}$. Direct calculation with the above given f_e yields

$$m_e n_e \langle v_x v_\beta \rangle = (n_{ce} T_c + n_{he} T_h) \left(\delta_{x\beta} + O(\alpha^2) \right) \quad (86)$$

where $\delta_{x\beta}$ is the Kronecker symbol ($\beta = x: \delta_{x\beta} = 1, \beta \neq x, \delta_{x\beta} = 0$). Below small corrections $O \sim \alpha^2$ are neglected. The components of Eq. (85) are given according to:

$$-\frac{1}{n_{ce}} \frac{\partial p_e}{\partial x} + e \frac{\partial \phi}{\partial x} = \frac{m_e}{\tau_{ce}} v_{ce x}, \quad en_{ce} E_y + \frac{e}{c} j_e B_0 \sin \alpha = 0, \quad e E_z = -\frac{m_e}{\tau_{ce}} v_{ce z} \quad (87)$$

with v_{ce} the velocity of the cold electrons, and $p_e = n_{ce}T_c + p_B$, $p_B = n_{he}T_h + B_y^2/8\pi$. For obtaining p_B Eq. (3) was used to eliminate j_e . The second equation only used for obtaining E_y . Using the first of Eq. (87) and Eq. (33) the pressure balance equation for the collisional region is obtained:

$$(1 + 1/\bar{Z})n_{ce}T_c + p_B = p_c^{-\infty} \quad (88)$$

with $p_c^{-\infty} = (1 + 1/\bar{Z})n_{ce}^{-\infty}T_c$, $n_{ce}^{-\infty}$ the value of n_{ce} in the depth of the plasma shield where p_B vanishes. At $x = L$ hot electrons and ions as well as the external magnetic field participate in the pressure balance from the side of the hot pre-sheath. Due to the small impact angle α hot ions don't bring substantial longitudinal momentum to the boundary. Therefore it is obtained:

$$n_{hi}^{\infty}H_0 \sin^2 \theta_0 + n_{he}^{\infty}T_h + (B_y^L)^2/8\pi = p_c^{-\infty} \quad (89)$$

Using Eq. (88) n_{ce} and p_e are expressed via p_B according to

$$n_{ce} = n_{ce}^{-\infty} - p_B / \left((1 + 1/\bar{Z})T_c \right), \quad p_e = n_{ce}^{-\infty}T_c + p_B / (Z + 1) \quad (90)$$

By substituting Eqs. (90) into the first of Eq. (87) it is obtained:

$$e\partial W/\partial x = m_e v_{cex}/\tau_{ce} \quad (91)$$

with W given as:

$$W = \phi - \phi_L + (T_c/eZ) \ln \left((p_c^{-\infty} - p_B) / (p_c^{-\infty} - p_B^L) \right) \quad (92)$$

W defines a new artificial potential which replaces the electric potential ϕ .

With the x- and z-components of the electron flux:

$$n_{ce}v_{cex} + j_{he} \sin \alpha = 0, \quad n_{ce}v_{cez} + j_{he} \cos \alpha = j_e \quad (93)$$

it is obtained from Eq. (91):

$$\frac{\partial W}{\partial x} = \theta \frac{m_e \sin \alpha}{en_{ce}\tau_{ce}} \frac{v_{The} n_{he}^{\infty}}{2\sqrt{\pi}} e^{-u_L} e^{\frac{e\Delta\phi}{T_h}}, \quad W(L) = 0, \quad (94)$$

$$u_L = -e\phi_L/T_h, \quad \Delta\phi = \phi - \phi_L = \phi - \phi_L + \text{ctg}\alpha \int_x^L E_z(x') dx' \quad (95)$$

Eq. (94) for W contains E_z (via $\Delta\phi$). Combining the third of Eq. (87) and Eqs. (91), (93) it is obtained:

$$E_z = (v_m/c) \partial B_y / \partial x - \text{ctg}\alpha \partial W / \partial x, \quad \int_x^L E_z dx = W \text{ctg}\alpha + (v_m/c) (B_y^L - B_y) \quad (96)$$

with $v_m = e^2/4\pi\sigma$ the magnetic diffusion coefficient. For small α and eliminating E_z from Eq. (95) it is obtained

$$\Delta\varphi = \frac{W}{\alpha^2} + \frac{v_m}{c\alpha} (B_y^L - B_y) \quad (97)$$

Then from Eqs. (4) and (96) follows for B_y :

$$\frac{\partial B_y}{\partial t} = \frac{\partial^2}{\partial x^2} \left(v_m B_y - \frac{cW}{\alpha} \right), \quad B_y(t=0) = 0 \quad (98)$$

The boundary condition at $x = -\infty$ is $B_y = 0$. To obtain another boundary condition for Eq. (98) the continuity of E_z at $x = L$ is used what means $E_z(L-0) = E_z(L+0)$. Then from Eqs. (83) and (96) it follows:

$$\frac{\partial}{\partial x} \left(\frac{v_m}{c} B_y - \frac{W}{\alpha} \right)_{x=L} = -\frac{1}{c} \dot{B}_y^L \quad (99)$$

For an analysis of the system of Eqs. (94), (95), (97) and (98) it is convenient to use the dimensionless variables:

$$u = -e\varphi/T_h, \quad w = -eW/(T_h\alpha^2), \quad (100)$$

$$b = B_y/B_y^0 \quad \text{with} \quad B_y^0 = cT_h\alpha/(v_m e), \quad (101)$$

$$\xi = (L-x)/\delta \quad \text{with} \quad \delta = \lambda_{he}\alpha, \quad \tau = t/t_0 \quad \text{with} \quad t_0 = l\delta/v_m \quad (102)$$

Then finally the following equations are obtained:

$$\partial w/\partial \xi = K \exp(u_L - u - \xi), \quad w(0) = 0, \quad u = u_L + w + b - b_0, \quad (103)$$

$$\mu \partial b/\partial \tau = \partial^2 (b+w)/\partial \xi^2, \quad b|_{\tau=0} = 0, \quad \partial(b+w)/\partial \xi|_{\xi=0} = \dot{b}_0, \quad b(\infty) = 0 \quad (104)$$

with $b_0 \equiv b(0)$, $\mu = \delta/l$ and the parameter K as given by Eq. (44). There is analogy between Eqs. (43) and (103).

A stationary solution of Eq. (104) ($\partial b/\partial \tau = 0$, $\dot{b}_0 = 0$) is $b+w = b_0$. Then from Eq. (103) it follows $w = (1-e^{-\xi})K$ and $b = Ke^{-\xi}$. The relaxation time τ_{st} to the stationary solution in case of small μ can be obtained keeping only $b_0 \neq 0$ in Eq. (104). Due to the smallness of μ the term $\mu \partial b/\partial \tau$ is neglected for every τ . Then it follows $b+w = b_0 + b_0\xi$ and the solution of the system of the Eqs. (103) and (104) becomes:

$$w = \left(1 - \exp\left(-\left(1 + \dot{b}_0\right)\xi\right) \right) K / \left(1 + \dot{b}_0 \right), \quad b = b_0 + \dot{b}_0\xi - w \quad (105)$$

After neglectation of the time derivation term in Eq. (104) the boundary condition $b(\infty)=0$ cannot be satisfied. Instead of that the physically reasonable condition $b(\xi_m) = 0$ with ξ_m the position of the minimum of the function $b(\xi)$ will be required. Derivation of b in Eq. (105) results in:

$$\xi_m = \ln(K/\dot{b}_0)/(1 + \dot{b}_0) \quad (106)$$

ξ_m expresses the thickness of the layer of the electric current via maximum value of time derivation of the magnetic field. From Eq. (105) at $\xi = \xi_m$ the following equation for b_0 is obtained:

$$b_0 = (K - \dot{b}_0 - \dot{b}_0 \ln(K/\dot{b}_0))/(1 + \dot{b}_0) \quad (107)$$

From Eq. (107) the behavior of b is obtained. For small time it follows $\dot{b}_0(0) = K$, i.e. for $b(0) = 0$: $b(\tau) = K\tau + o(\tau)$. The small term $o(\tau)$ is obtained from the Taylor series expansion of Eq. (107) at the point $\dot{b}_0 = K$:

$$b_0 = \frac{1}{2}(1 - \dot{b}_0/K)^2/(1 + 1/K) + \dots,$$

therefore $\dot{b}_0 \approx K(1 - \sqrt{2 + 2/K} \sqrt{K\tau + o})$. Thus it is obtained

$$b_0 \approx K\tau - \sqrt{\frac{8}{9}}(K\tau)^{3/2}, \quad \tau \ll 1/K \quad (108)$$

The relaxation time is estimated at $\dot{b}_0 \ll K$. From Eq. (107) with $b_0 \approx K/(1 + \dot{b}_0)$ it follows $b_0 \approx K(1 - e^{-\tau/K})$ at $\tau > K$, i.e. $\tau_{st} = K$. As will be shown below this relaxation is too long for our applications. The stationary regime with small μ is not needed. If $\tau \ll K$ then $b_0 \ll K$ and at $1 \ll \dot{b}_0 \ll K$ it is valid $b_0 \dot{b}_0 \approx K$, then it follows:

$$b_0 = \sqrt{2K\tau}, \quad 1/K \ll \tau \ll K \quad (109)$$

With the help of Eq. (103) w can be expressed via b according to:

$$w = \ln\left(1 + K \int_0^\xi e^{b_0 - b(\xi') - \xi'} d\xi'\right) \quad (110)$$

Omission of b ($b \ll 1$) in Eq. (110), and integration of this equation results in:

$$w = \ln\left(1 + K(1 - e^{-\xi})\right) \quad (111)$$

again in analogy to Eq. (45). From Eqs. (100) and (111) at $\tau \ll 1/K$ the drop of W in the collisional region is obtained as $-eW_{\max} = \alpha^2 T_h \ln(1+K) \ll T_h$. This drop is much less than for the perpendicular case. From Eq. (92) the same conclusion follows for the usual electric potential: $-e\Delta\phi \ll T_h$, i.e. while electrical stopping at $\alpha \ll 1$ is important it occurs due to the vortex electric field. The criterion for electrical stopping is $\xi_m < 1$. Using Eqs. (106), (108) and (109) it is obtained:

$$\xi_m \approx \left(\sqrt{\frac{2\tau}{K}} \text{ at } \tau < \frac{1}{K}, \quad \frac{\sqrt{2\tau K}}{K} \ln \sqrt{2\tau K} \text{ at } \frac{1}{K} \ll \tau \ll K, \quad 1 \text{ at } \tau \geq K \right) \quad (112)$$

there is no electrical stopping effect for $\tau > K$, i.e. for regimes which are close to the stationary one. The term with μ in Eq. (104) can be neglected if the inductance of the transition region is larger than that of the current layer, i.e. if $1 \gg \delta\xi_m$, hence it should be $\mu\xi_m \ll 1$ (This can be checked directly by comparing terms in Eq. (104)).

Using for estimations the plasma parameter $\beta = 8\pi p_h^\infty / B_0^2$ with $p_h^\infty = 2n_{he}^\infty T_h$, $n_{hi}^\infty H_0 \sin^2 \theta_0 = n_{he}^\infty T_h$, the pressure balance condition (89) and assuming $\bar{Z} \gg 1$ it is obtained from Eqs. (101), (102) and (39):

$$\frac{t_0}{\tau_{he}} \approx \frac{1}{8} \alpha^2 \beta \left(\frac{\omega_e \tau_{he}}{1 + q_b} \right)^2 \frac{\varepsilon^7}{\bar{Z}^3 \mu}, \quad \mu = \frac{\alpha \tau_{he} v_{The}}{2(1 + q_b)} \frac{\varepsilon^2}{\bar{Z}}, \quad \frac{B_y^L}{B_0} \approx \frac{1}{4} b_0 \alpha \beta \omega_e \tau_{he} \frac{\varepsilon^3}{\bar{Z}} \quad (113)$$

with $q_b = (1/\beta)(B_y^L/B_0)^2$. The parameter q_b shows the ratio of the additional magnetic pressure to the pressure of the hot plasma.

For typical ITER conditions²⁰ with:

$$n_{he}^\infty = 3.10^{13} \text{ cm}^{-3}, \quad T_h = 10 \text{ keV}, \quad B_0 = 5 \text{ T}, \quad \alpha = 0.1 \text{ rad}, \quad l = 5 \text{ cm}$$

it is obtained from Eq. (28):

$$v_{hi}^L = 6\bar{Z}T_h^2 \lambda_{hi} / \left(\lambda_{he} m_i m_t v_c^3 \right), \quad v_{The} \approx 5 \cdot 10^9 \text{ cm/s}, \quad \beta \approx 0.01, \quad \omega_e \approx 10^{12} \text{ s}^{-1}.$$

For the corona with $T_c = 10^2 \text{ eV}$ (i.e. $\varepsilon = 0.1$), $\bar{Z} = 6$ (see Sec. 2), and $K=7$ (see Table 2), it is obtained $B_y^L/B_0 = 40b_0$, $\mu = 100$, $t_0 \approx 0.03 \text{ s}$. As follows from $\mu\xi_m < 1$ and from Eq. (112) it is estimated for the corona $\tau < 10^{-4}$, i.e. $t < 10^{-5} \text{ s}$ - initial phase of disruption. During this phase it is obtained from Eq. (108): $b_0 = K\tau < 10^{-3}$, i.e. $B_y^L/B_0 < 0.03$. Hence for the initial phase the condition of small additional magnetic field in the corona is satisfied. The cold plasma perturbation by the pressure gradient of the magnetic field is rather small ($q_b = 0.2$). The thickness of the electric layer $\delta\xi_m$ is smaller than l , it can be less than that of the corona.

If the corona region is too thin or if it is absent then electrical stopping by the LTE plasma has to be analyzed. Taking $T_c = 4 \text{ eV}$ (i.e. $\varepsilon = 0.02$), $\bar{Z} = 3$, it is obtained $B_y^L/B_0 = 0.7b_0$, $q_b = 10^2 b_0^2$, $\mu = 8/(1 + q_b)$, $t_0 [\text{s}] \approx 10^{-5} / (1 + q_b)$, $K = 20$ (from Eq. (55) $K \propto Z/\varepsilon$). The inequality $\mu\xi_m < 1$ is satisfied: with the increase of τ the left hand side of this inequality gets larger up to ~ 0.05 at $\tau \sim 0.005$ but at larger τ again gets smaller. After a short time ($t < 1 \mu\text{s}$) the approach used cannot be applied anymore: $b_0 \sim 1$, i.e. $B_y^L \sim B_0$.

The estimation at $q_b > 1$ is not fully correct, because in Eqs. (113) there is assumed a dynamically changing value of b_0 in time for μ and t_0 . A first consequence of the rise of B_y is a magnetic prevention of expansion of the vaporized cold plasma from the target. A correct description should include the development of a shock wave as a

result of magnetic compression in the course of increasing B_y . Such physical picture of electrical stopping in a LTE plasma is similar to that of a Z-pinch discharge in presence of a longitudinal magnetic field: a strong current flowing in a relatively thin skin-layer of the plasma conductor leads to radial self-compression of the column. While $B_y \ll B_z$ the Suydem stability criterion²¹ has to be satisfied. Therefore the compression can be stable up to times when B_y reaches $B_y \sim B_0$. At that time a decrease of the hot electron collisional stopping length λ_{he} due to some anomalous mechanism could occur. The anomalous stopping length can be found from the condition $B_y^L = B_0$ at the stationary regime. To support or reject such speculations experimental results are needed. Magnetic contraction of the shielding layer at $B_y^L < B_0$ can form a cord-like shape of the cold plasma requiring another mathematical model of process.

Up to now only the initial phase of a disruption with formation of a corona was analyzed. For larger times the situation corresponding to intermediate and large values of μ should be considered. In this case the term $\mu \partial b / \partial t$ should be taken into account in Eq. (104). At the end of the initial phase a relatively small value of b with $b \sim 10^{-3}$ is obtained. Therefore the solution (111) of Eq. (103) can be used for $w(\xi)$. Eq. (104) is rewritten in terms of the function $g = b + w$. Because of $\partial g / \partial \tau = \partial b / \partial \tau$ the standard problem for a parabolic equation is obtained:

$$\mu \frac{\partial g}{\partial \tau} = \frac{\partial^2 g}{\partial \xi^2}, \quad g|_{\tau=0} = w, \quad \left. \frac{\partial g}{\partial \xi} \right|_{\xi=0} = \dot{b}_0, \quad g(\infty) = w(\infty) \quad (114)$$

In terms of b the formal solution of Eq. (114) becomes²²:

$$b(\tau, \xi) = \frac{1}{2} \sqrt{\mu/\pi\tau} \int_0^\infty w(\xi') \sum \exp\left(-\mu(\xi' + \sigma\xi)^2/4\tau\right) d\xi' - \int_0^\tau (\pi\mu(\tau - \tau'))^{-1/2} \exp\left(-\mu\xi^2/4(\tau - \tau')\right) \dot{b}_0(\tau') d\tau' - w(\xi) \quad (115)$$

This is still not the final solution because Eq. (115) includes the unknown function \dot{b}_0 . The dependence of $b(\tau, 0)$ on τ conveniently is represented as $b_0 = Kf(\mu\tau)/\mu$. Then from Eq. (115) it follows the integral equation for the function f :

$$\sqrt{\pi} f(x) + \int_0^x \frac{df(y)}{dy} \frac{dy}{\sqrt{x-y}} = \frac{2\mu}{K} \int_0^\infty w(2y\sqrt{x}/\mu) \exp(-y^2) dy \quad (116)$$

with $x = \mu\tau$. Eq. (116) is a Volterra type equation. At small arguments $\xi = 2y\sqrt{x}/\mu$ the function w is represented with the first term of the Taylor expansion: $w \approx K\xi$ at $\xi \ll 1/K$. The function under the integral at the RHS has to be evaluated in the interval $0 < y < Y$ with $Y \sim 1$. The case $\xi \ll 1/K$ corresponds to $\tau \ll \mu/4K^2$, i.e. for the corona to $t \ll 0.1$ s. Then for the value of the RHS it is obtained $2\sqrt{x}$. Laplace transformation of Eq. (116) and use of standard tables of reverse functions results in the following solution:

$$f(x) = (1/2\pi i) \int_{\sigma-i\infty}^{\sigma+i\infty} s^{-3/2} (1+s^{1/2})^{-1/2} e^{xs} ds = 2\sqrt{x/\pi} - 1 + e^x \operatorname{erfc}\sqrt{x} \quad (117)$$

Table 3 lists the calculated magnetic field for the corona with f of Eq. (117).

In the corona the approach described above can be used for times smaller than $t \sim 10^2 \mu\text{s}$. Later the value of B_y can reach that of B_0 as a result of magnetic field generation during electrical stopping. At the time when it is allowed to neglect the influence of the magnetic self-compression ($t < 10 \mu\text{s}$) the linear approximation $f \approx x$ is still valid, i.e. $b \approx K\tau$, hence it could be used either the relatively simple expression (105) at $\xi < \xi_m$ or the more complicated one (116). This can be used at every ξ to obtain the spatial dependence $b(\tau, \xi)$. From Eq. (103) the dependence of the effective potential drop on ξ is obtained as $\Delta u = w + b - b_0$. Comparing this expression with Eq. (105) it is obtained for $\Delta u = \dot{b}_0 \xi \approx K\xi$. This is quite the same as the behavior of the usual potential for perpendicular impact (the dependence on τ doesn't develop at this relatively small time). Therefore the energy deposition in the electrical stopping region can be described with that part of the curve of Fig. 6 (using the $\alpha\lambda_{he}$ -scale) which is adjacent to the point $x = L$, or with the formula:

$$dQ_e/dx \approx (KQ_e^L/\alpha\delta) \exp(K(x-L)/\alpha\delta). \quad (118)$$

A characteristic value of the uncompensated electric current can be estimated by using the cord-like conductor model with the cord radius l . For $l = 5 \text{ cm}$ and $B_y^L = 1 \text{ T}$ the current is given as:

$$I = (cl/4\pi) B_y^L 10^{-9}/3 \approx 30 \text{ kA}.$$

The time t_b of reaching the equality $q_b = 1$ depends on T_c . The scaling $t_b(T_c)$ follows from Eq. (113) providing a scaling of t_0 and b_0 at fixed B_y^L/B_0 :

$$t_0 \propto \varepsilon^5/\bar{Z}^2, \quad b_0 \propto \bar{Z}/\varepsilon^3.$$

The dependencies of values b_0 and K on the parameters are given as

$$b_0 \approx K t_b/t_0, \quad K \propto \bar{Z}/\varepsilon$$

Thus using the point $t_b(100\text{eV}) = 10 \mu\text{s}$ of Table 3 it is obtained $t_b[\mu\text{s}] = (T_c/10\text{eV})^{3/2}/3$.

For perpendicular impact the energy of the hot electrons deposited by collisional stopping into the plasma shield results in Joule heating of the reverse current of the cold electrons. For inclined impact only a part of the collisional energy deposition of the hot electrons is deposited in such a way. The other part is used for production of the magnetic field B_y . At the initial step when $\mu\xi_m < 1$ the external volume occupied by the magnetic field is much larger than the internal one in the plasma shield. In this case the Joule heating is small in comparison with the energy spent for magnetic field production. At $\mu\xi_m > 1$ the internal volume is becoming larger than the external one. In such a case approximately half of the energy is spent for production of the magnetic field²³. The energy estimated for Joule heating is given as:

$$Q_J(L) \approx Q_e(L) \frac{\mu\xi_m}{1 + 2\mu\xi_m}$$

A more correct calculation of the energy deposition into the shielding layer should account for the shock wave produced by the magnetic field gradient and requires additional considerations outside of this work.

In accordance with Eq. (84) and with the conclusion that $\varphi = 0$ in the transition region the potential part of the electric field at $x \approx L + r_{hi}$ is given as

$$E_x^L \approx -\partial\phi/\partial x \approx l\dot{B}_y^L/\alpha c$$

Then it follows for the drift velocity v_D^L :

$$v_D^L = c E_x^L / B_0 = (l/t_0\alpha) (B_y^0/B_0) db_0/d\tau \quad (119)$$

From Eq. (113) it is obtained: $B_y^0/B_0 = 40$, $db_0/d\tau = K$ for the corona. Hence for v_D^L is obtained $v_D^L \approx 5 \cdot 10^5$ cm/s. Shifting of the hot plasma coming from the core with such a velocity along the y-direction means that after $t = l/v_D^L = 10 \mu s$ the hot plasma impacts to a divertor area hitherto not hit by the hot plasma as is schematically shown in Fig. 8. This is an additional time limitation. Therefore a separate consideration of the drift shifting is important for understanding properly the dynamics of the electric drift of the hot plasma.

The difference of analyses of the the $\mathbf{E} \times \mathbf{B}$ drift to other drift models (see e.g. Ref. 24) is as follow: the problem considered concerns a fast non-stationary lateral shift of the SOL caused by the necessity to compensate the hot electrons unlimited acceleration by the vortex electric field in the SOL. The usual drift models concern drift effects of plasma fluxes along the SOL onto the divertor plates during quasi-stationary operational regime of tokamak. Only potential electric fields had been analyzed in the SOL which are caused by quite different physical reasons: by the longitudinal temperature gradient near the divertor plates or by the potential difference between the core plasma and the first wall which arise because of the different mobility of electrons and ions across the confining magnetic field.

6. THE MAGNETIC PRE-SHEATH AND THE ELECTROSTATIC SHEATH

The hot ion magnetic pre-sheath is located at $x > L$ outside of the cold plasma (see Fig. 3). The flux of hot ions is described by the distribution function (81). In order to obtain the criterion of applicability of the effective potential approximation for hot ions the change of the vortex electric field over the hot ion Larmor radius near the edge of the cold plasma (at $x = L$) is estimated. In accordance with Eqs. (80) and (83) the condition for this criterion is $r_{hi} \ll l$. This is well satisfied for the parameters of Sec. 5.2. Thus the same effective potential φ can be used both for electrons and ions. To calculate the value of the adiabatic invariant I for the region of $\varphi \neq 0$ the spatial behavior of the effective potential as shown in Fig. 9 is used. The aim is to calculate the value of φ_L . For the analysis of the ion pre-sheath zero thickness of the sheath (due to the fact that $r_D \ll r_{hi}$) and linear approximations of the dependence of the potential at $x > L$ in each cell of ion pre-sheath indexed with $j=1..J$ are used. The index L will be used only for φ_L . Hence the effective potential is approximated by:

$$\varphi(x) = \left[\varphi_L, x < x_0; \quad W_j + 2P_j x, x_{j-1} \leq x < x_j, j=1..J; \quad \varphi_j, x_j \leq x \right] \quad (120)$$

$$\text{with } P_j = \frac{1}{2}(\varphi_j - \varphi_{j-1})/(x_j - x_{j-1}), \quad W_j = \varphi_{j-1} - 2P_j x_{j-1}, \quad x_0 = L, \quad \varphi_j = 0$$

To describe the regions $x < L$ (the cell with $j = 0$) and $x \geq x_j$ (the cell with $j = J+1$) the definitions for P_j and W_j are extended to $W_0 = \varphi_L, P_0 = 0, W_{J+1} = 0, P_{J+1} = 0$.

Attention has to be given to some consequences of the potential jump at $x = L$. Due to this break the conservation of I at the moment when the trajectory of an ion touches the sheath (i.e. after minimal position of ion oscillation motion x_{\min} has approached to $x = L$: $x_{\min} \leq L$) is not valid because after this moment there occurs a significant change of the transversal projection during one cycle of transversal motion. The value of H_{\perp} should be constant at this cycle but the value of the adiabatic invariant gets some definite increment ΔI (being calculated below). As a result it is taken $I = I_0$ if the transversal projection is $x_{\min} > L$ and $I = I_0 + \Delta I$ for $x_{\min} \leq L$, i.e. Eq. (81) in the (X, Z) -frame is transformed to

$$f_{hi} = C_i \delta(H - H_0) \delta\left(I - I_0 - \Delta I \theta\left(X_c^{(0)} - X_c\right)\right) \quad (121)$$

with $\theta(s) = (0, s < 0; 1, s \geq 0)$ and $X_c^{(0)}$ the leading center position corresponding to $x_{\min} = L$. Considering the transversal projections of the trajectory at $Z = 0$, final results are valid for each Z due to symmetry. The projections are determined either by the parameter X_{\min} or X_{\max} which depend on X_c . To shorten the expressions the following dimensionless variables (neglecting the difference between $\cos\alpha$ and 1) are used:

$$w = -e\varphi/I_0, \quad w_j = -e\varphi_j/I_0, \quad w_L = -e\varphi_L/I_0, \quad \bar{w}_j = -e W_j/I_0, \\ p_j = -e r_{hi} P_j/I_0, \quad s = (X - L)/r_{hi}, \quad i = I/I_0, \quad h = H_{\perp}/I_0$$

Hence from Eq. (120) it is obtained:

$$w(s) = w_L, s < s_0; \quad \bar{w}_j + 2p_j s, s_{j-1} \leq s < s_j, j=1..J; \quad w_j, s_j \leq s (w_j = 0), \\ p_j = \frac{1}{2}(w_j - w_{j-1})/(s_j - s_{j-1}), \quad \bar{w}_j = w_{j-1} - 2p_j s_{j-1}, \quad (122) \\ \bar{w}_0 = w_L, \quad p_0 = 0, \quad \bar{w}_{J+1} = 0, \quad p_{J+1} = 0$$

Applying also the following designations:

$$\Theta_j = \bar{w}_j + (p_j + 2s_c) p_j \quad (s_c = (X_c - L)/r_i) \\ \Omega(a) = (2/\pi) \int_0^a \sqrt{1 - z^2} dz = \pi^{-1} \left(\arcsin a + a \sqrt{1 - a^2} \right), \\ \bar{s}_j = \left[(s_{\min}, j = j_{\min} - 1), \quad (s_j, j_{\min} \leq j < j_{\max}), \quad (s_{\max}, j = j_{\max}) \right]$$

with j_{\min}, j_{\max} the indexes of the boundary cells of the trajectory projection location. It is valid $0 \leq j_{\min} \leq j_{\max} \leq J+1$. For the general expression for i is finally obtained:

$$i = \frac{2}{\pi} \sum_{j=j_{\min}}^{j_{\max}} \int_{\bar{s}_{j-1}}^{\bar{s}_j} \sqrt{h + \bar{w}_j + 2p_j s - (s - s_c)^2} ds = \sum_{j=j_{\min}}^{j_{\max}} (h + \Theta_j) \Omega(a) \Big|_{a'_j}^{a_j}, \quad (123)$$

with $a_j = (\bar{s}_j - s_c - p_j) / \sqrt{h + \Theta_j}$, $a'_j = (\bar{s}_{j-1} - s_c - p_j) / \sqrt{h + \Theta_j}$,

with the designation $f(x)|_a^b \equiv f(b) - f(a)$ and with S_{\min} and S_{\max} given as:

$$s_{\min} = s_c + p_{j_{\min}} - \sqrt{h + \Theta_{j_{\min}}}, \quad s_{\max} = s_c + p_{j_{\max}} + \sqrt{h + \Theta_{j_{\max}}}$$

The indexes j_{\min} and j_{\max} are determined from the condition that they bound the region $-1 \leq a'_j < a_j \leq 1$. They can easily be found numerically.

Simplest types of projections:

1. (deeply in the hot pre-sheath)

$$s_j \leq s_{\min} : i = 1, \quad j_{\min} = j_{\max} = J + 1, \quad \Theta_{J+1} = p_{J+1} = 0, \quad \Omega(\pm 1) = \pm \frac{1}{2},$$

$$i = h, \quad s_{\min} = s_c - \sqrt{h}, \quad s_{\max} = s_c + \sqrt{h}.$$

2. (deeply in the cold pre-sheath)

$$s_{\max} < 0 : i = 1 + \Delta i, \quad j_{\min} = j_{\max} = 0, \quad \Theta_0 = w_L,$$

$$i = h + w_L, \quad s_{\min} = s_c - \sqrt{h + w_L}, \quad s_{\max} = s_c + \sqrt{h + w_L}$$

$s_c^{(0)}$ defined by $s_c^{(0)} = (x_c^{(0)} - L)/r_i$ is obtained from the equation

$$h + \bar{w}_1 + 2p_1 s_{\min} - (s_{\min} - s_c)^2 = 0$$

at $s_{\min} = 0$. Substituting the result $s_c^{(0)} = \sqrt{h + \bar{w}_1}$ into Eq. (123) for $j = j_{\min} = 0$ yields the following expression for Δi :

$$\Delta i = \left(\frac{1}{2} - \Omega \left(\sqrt{(h + w_0)/(h + w_L)} \right) \right) (h + w_L) \quad (124)$$

For small differences $\varphi_L - \varphi_0$ it is obtained $\Delta i \propto (\varphi_L - \varphi_0)^2$.

From Eqs. (74) and (121) after transformation to dimensionless variables it is obtained:

$$n_{li}(s) = n_{li}^{\infty} \frac{\cos \theta_0}{2\pi} \int_0^{2\pi} d\eta \int_0^{\infty} dh \delta(i - 1 - \Delta i \theta(s_c^{(0)} - s_c)) (1 - h \sin^2 \theta_0)^{-1/2} \quad (125)$$

with η the angle of the perpendicular velocity polar coordinates $v_x = v_{\perp} \cos \eta$, $v_y = v_{\perp} \sin \eta$. When carrying out the integrating over h , η should be fixed. The relation between h and s_c follows from the expression $p_y - m_i \omega_i X = m_i v_y$:

$$s_c(h) = s + \sqrt{h + w(s)} \sin \eta \quad (126)$$

The dependency under the integral in Eq. (125) on η is only implicitly via $\sin\eta$ in s_c of Eq. (126). Due to this if integrating over $d\eta$ from 0 to 2π the integration is repeated two times. Hence it is sufficient to integrate over $d\eta$ from $-\pi/2$ to $\pi/2$ (thus having only positive sign of $\cos\eta$). Replacing the variable h by i and performing the internal integration it is obtained

$$n_{hi}(s) = n_{hi}^{\infty} \pi^{-1} \cos\theta_0 \int_{-\pi/2}^{\pi/2} \left(1 - h \sin^2 \theta_0\right)^{-1/2} (di/dh)^{-1} d\eta \quad (127)$$

with h the solution of the equation

$$i(h, s_c(h)) = 1 + \Delta i(h) \theta \left(\sqrt{h + \overline{w}_1} - s_c(h) \right) \quad (128)$$

For the derivation di/dh it is obtained:

$$\frac{di}{dh} = \frac{1}{\pi} \sum_{j=j_{\min}}^{j_{\max}} \left(\arcsin(a) \Big|_{a_j}^{a_j} - \sin \eta \sqrt{(h + \Theta_j)/h + w(s)} \sqrt{1 - a^2} \Big|_{a_j}^{a_j} \right) \quad (129)$$

In particular for the above mentioned simplest types of projections 1 and 2 it is obtained $di/dh = 1$, i.e. the relation of ion densities for both sides of the whole potential sheath:

$$n_{hi}^{\infty} / n_{hi}^{-\infty} = \sqrt{1 - \Delta i \tan^2 \theta_0}$$

The usual potential ϕ in the ion pre-sheath is found from the quasineutrality equation:

$$n_{hi} = n_{he} + n_{ce}. \quad (130)$$

The electric current of cold electrons compensates the current of the hot electrons. The current of hot ions is neglected. To calculate the potential in the sheath the Poisson equation for ϕ has to be solved. Due to the fact that the vortex part of the electric field is smooth at $x = L$ the Poisson equation can be formally applied for the effective potential:

$$d^2\phi/dx^2 = 4\pi e(n_{he} + n_{ce} - n_{hi}), \quad \phi(-\infty) = \phi_L, \quad \phi(+\infty) = \phi_0 \quad (131)$$

with designations " $-\infty$ " and " $+\infty$ " denoting the conditions at the conventional boundaries of the sheath which are assumed to be infinitely far because of the zero approximation for the small parameter r_D/r_{hi} .

The calculation for the ion pre-sheath, like that for the collisional region, needs as only external unknown parameter $u_L = -e\phi_L/T_h$. u_L will be obtained after solution of the sheath problem (131). From the condition of zero electron current $j_{he} + j_{ce} = 0$ according to Eqs. (20), (26) it is obtained $n_{ce}^{\infty} = n_{he}^{\infty} e^{-u_L} / 2\sqrt{\pi u_L}$. Quasineutrality at $x \rightarrow \infty$: $n_{hi}^{\infty} = n_{he}^{\infty} + n_{ce}^{\infty}$ in accordance with Eqs. (19), (32), (52), (25) or (127) gives $n_{he}^{\infty} = qn_{hi}^{\infty}$. After this Eq. (131) for the dimensionless potential $u(s) = -e\phi/T_h$ has the form:

$$d^2u/d\zeta^2 = \delta n, \quad u(-\infty) = u_L, \quad u(+\infty) = u_0, \quad (132)$$

$$\delta n = \frac{\cos \theta_0}{\pi} \int_{-\pi/2}^{\pi/2} \frac{d\eta}{\sqrt{1 - h \sin^2 \theta_0}} \frac{di/dh}{\pi \left(e^{-u} k(u_L - u) + e^{-u_L} / 2 \sqrt{\pi u_L (1 - u/u_L)} \right)}$$

with $\zeta = (X - L)/r_D$, h and di/dh given by Eqs. (128) and (129). For solving the problem of the quasi neutral ion pre-sheath it is assumed $\delta n = 0$. The following relation is valid between the dimensionless potentials u and w : $u = Gw$ with $G = I_0/T_h$.

In the narrow sheath it is allowed to neglect the explicit dependency in the left term of the RHS of Eq. (132) on ζ but the dependency of the ion density on u has to be kept. Therefore Eq. (132) can be integrated over ζ from $\zeta = -\infty$ to $\zeta = +\infty$ with the weight function $du/d\zeta$ thus obtaining the equation for u_L :

$$B_y^0 / B_0 = 40 \quad (133)$$

The system of equations (130), (132), and (133) has been solved numerically. The results of this calculation for the pitch-angle $\theta_0 = \pi/4$ and $G=2$ are presented in Figs. 10 and 11, showing the dependencies of the dimensionless potential $u(\xi)$, $u(\zeta)$ both for the sheath and for the ion pre-sheath as well as the densities of the ions and the electrons there. Results of calculations performed for different values of G are listed in Table 4.

It was also checked numerically that the Bohm criterion is valid for the points of the Table 4, but not for smaller values of G . The main drop of the potential occurs in the sheath providing the values of $\varphi_L = -T_h u_L / e$ which cannot change the value of the parameter K significantly. Therefore the estimations in Sec. 5.2 for $K = 7$ are confirmed by the analysis of the current part.

The behavior of the effective potential is rather close to that one for perpendicular impact if the spatial coordinate is shortened by the factor $\sin \alpha$ with α the inclination angle. According to Fig. 11 the potential in the ion pre-sheath changes only slightly in contrast to the case of the traditional ion pre-sheath problem^{8,10} where the main potential drop occurs in the pre-sheath because the absorption of ions at the solid wall decreases their density significantly. For inclined impact ions cannot be absorbed immediately by the cold plasma because their stopping range λ_{hi} is assumed to be much larger than their full path of immersion into the cold plasma. Thus their density doesn't decrease significantly in the ion pre-sheath region. The Bohm criterion is valid if $G_\perp = G \sin \eta > 1,75$ with η the pitch angle of the mono-energetic hot ions at $x = \infty$. To fulfill this condition acceleration of the hot ions in the hot pre-sheath is required⁹.

7. CONCLUSIONS

Potential profiles have been calculated for perpendicular and inclined impact of hot plasma. In terms of effective potential the results are identical. However there are important differences in the behavior of the electric potential of both cases as is schematically indicated in Fig. 12. In case of perpendicular impact of hot plasma the main electric potential drop occurs in the rather narrow hot electron collision stopping region (see curve 1 of Fig. 12). The electric field created by this potential drop

effectively stops the hot plasma electrons. Their energy deposition into the main volume of the plasma shield amounts only up to 10 %.

In case of inclined impact of the hot plasma an effective potential being the sum of the electric potential and a vortex term has to be introduced (see curve 2 of Fig. 12). In the electric drift region the effective potential is zero thus the electric potential compensates the vortex term. The rather large electric potential drop gives rise to an electric field there which causes a drift of the hot plasma in lateral direction. The electric potential drop $\Delta\phi$ in the collisional region is proportional to α^2 and thus is rather small in comparison with the potential drop for perpendicular impact. Generally the increase of inclination of the confining magnetic field leads to a decrease of the role of the electric potential in the shielding layer and to an increase of the role of the vortex electric field for the stopping of hot electrons.

In case of inclined impact of hot plasma an electric current is produced which leads to the generation of an additional magnetic field B_y in the plasma shield. The increase of the magnetic pressure gradient caused by B_y could result in a self compression of the edge of the plasma shield at times comparable or smaller than the characteristic disruption time. B_y thus becomes a substantial feature of the expansion of the plasma shield. Therefore the dynamics of the cold plasma shield is influenced by the time evolution of B_y . For evolution of the shielding efficiency of the plasma shield the self compression of the edge of the shielding layer by the magnetic field B_y and the dynamics of the $\mathbf{E} \times \mathbf{B}$ drift of the hot plasma still have to be studied in detail.

The characteristic time of development of important effects predicted by the model is much less than the disruption time (the increase of magnetic pressure due to additional magnetic field component B_y up to the value of plasma pressure and lateral drift shift of the incoming hot plasma flux in the vicinity of cold plasma up to the value of the SOL thickness happens on time scales of 10^{-5} s in accordance with the results of analysis carried out in Sec. 5.2 and shown in the Table 3 and in the last paragraph of the section). This circumstance gives additional argument for the use of tokamak parameters as input for the model. The model is valid as long as the additional magnetic field is less than the guiding magnetic field, for the corona this time is of the order of the disruption time 10^{-4} s. The small characteristic time leads to the conclusion that calculations of the hot plasma-target interaction resulting in the target erosion should take into account magnetic self-compression and lateral electric drifts.

7. ACKNOWLEDGEMENT

The authors would like to thank Sergey Pestchanyi from TRINITY Troitsk for fruitful discussions and participation at the initial stage of this work and Heide Hofmann from FZK Karlsruhe for her patience in typewriting the manuscript.

8. REFERENCES

- ¹A. Sestero, Nuclear Fusion, Vol. 35 (1995), 919.
- ²H. Würz, I.Landman, B.Bazylev, F.Kappler, G.Piazza, S.Peschannyi, J. Nucl. Mater., Vol. 233 - 237 (1996), 798.
- ³R. Aymar, Fusion Eng. And Design, Vol. 36 (1997), 9.
- ⁴H. Würz, N.Arkipov, V.Bakhtin, I.Konkashbaev, I.Landman, V.Safronov, D.Toporkov, A.Zhitlukhin, J. Nucl. Mater. Vol. 220 - 222 (1995), 1066.

- ⁵I. Landman, H. Würz, In 24th Conference on Controlled Fusion and Plasma Physics (European Physical Society, Berchtesgaden, 1997), Vol.21A, Part IV, p.1821.
- ⁶G.D.Hobbs, J.A.Wesson, Plasma Physics, Vol. 9 (1967), 85.
- ⁷P.C. Stangeby, In Physics of Plasma-Wall Interactions in Controlled Fusion edited by D.E. Post and R. Behrisch (Plenum Press, New York, 1986), p. 41.
- ⁸R. Chodura, *ibida* p. 99.
- ⁹K.U. Riemann, J. Phys. D, Appl. Physics, Vol 24 (1991), 493.
- ¹⁰D.D. Ryutov, Contrib. Plasma Phys. Vol 36, 2/3 (1996), 20.
- ¹¹L.L. Lengyel, V.A. Rozhansky, I.Yu. Veselova, Nucl. Fusion, Vol 36 (1996), 1679.
- ¹²L.L. Lengyel, V.A. Rozhansky, I.Yu. Veselova, P.J. Lalouis, Nucl. Fusion, Vol 37 (1997), 1245.
- ¹³S.Pestchanyi, H. Würz, B.Bazylev, F.Kappler, I.Landman, In 24th Conference on Controlled Fusion and Plasma Physics (European Physical Society, Berchtesgaden, 1997), Vol.21A, Part III, p.981.
- ¹⁴H. Würz, B.Bazylev, F.Kappler, I.Landman, S.Peschannyi, G.Piazza, Fusion Technology 1996, edited by C.Varandas and F.Sierra, Vol.1, p.191.
- ¹⁵The electrical stopping was approximately taken into account by assuming that ions and electrons contribute equally to the deposited energy.
- ¹⁶The collisional region consists of the main volume of the cold plasma shield and of the electrical pre-sheath.
- ¹⁷S.I.Braginskij. Transport phenomena in plasmas. In: 'The problems of plasma theory' edited by M.A.Leontovitch, 'Atomizdat', Vol.1 (1963), p.183 (in Russian).
- ¹⁸F.Hinton, In Basic plasma physics I, Editors A.A. Galeev, R.N.Sudan, North-Holland Publishing Company, 1983.
- ¹⁹L.D.Landau, E.M.Lifshits. Mechanics. The course of theoretical physics, 'Nauka', Vol. 1 (1973), (in Russian).
- ²⁰D.E.Post (ed), ITER Physics, ITER Documentation Series, No.21, Chapter 4 (IAEA, Vienna, 1990).
- ²¹B.K. Suydem, TID/7558 Conf. on Controlled Thermonuclear, Fusion Washington, DC Feb. 3/5, 1958.
- ²²L.D.Landau, E.M.Lifshits. Hydrodynamics. The course of theoretical physics, 'Nauka', Vol. 6 (1986), (in Russian).
- ²³H. Knöpfel, Pulsed high magnetic fields, North Holland Publishing Company 1970.
- ²⁴P.C.Stangeby, A.V.Chankin. Nuclear Fusion, Vol. 36 (1996), 839.

Table 1. The dependence of the sheath potential on the dimensionless energy G of the incoming hot ions.

G	0.55	1	2	5
u_L	0.90	0.69	0.58	0.52
G_{\min}	0.54	0.57	0.60	0.63

Table 2. Typical values of the dimensionless parameters

$G = 1$	$\gamma = 1/70$	$\bar{z} = 6$	$\varepsilon = 1/10$
$q = 0.95$	$q_e = 0.16$	$q_i = 1.77$	
$y = 0.076$		$u_{\infty} = 2.8$	
	$= 7.28$		
$Q_{e0} = 11\%$	$Q_{eL} = 81\%$	$Q_i = 8\%$	

Table 3. Typical dynamics of the additional magnetic field (for $t_0=0.03$ s, $\mu=100$, $K=7$, $\beta=0.01$)

time [s]	10^{-5}	$3 \cdot 10^{-5}$	10^{-4}
$x = \mu t/t_0$	0.04	0.12	0.4
$f(x)$	0.034	0.1	0.27
b_0	$2 \cdot 10^{-3}$	$7 \cdot 10^{-3}$	$2 \cdot 10^{-2}$
B_y^L/B_0	0.08	0.3	0.8
q_b	0.6	9	64

Table 4. Results of calculations for electrostatic sheath and ion pre-sheath

G	1.75	2	3.5
u_L	0.79	0.73	0.57
u_0	0.095	0.082	0.043

Figures captions:

- Fig. 1: Density distributions of the cold and hot plasma ions (n_{ci} , n_{hi}) and electrons (n_{ce} , n_{he}). $x < 1$: λ_{he} - units, $x > 1$: $10 r_D$ - units.
- Fig. 2: Dimensionless potential and particle fluxes in the cold ($x < 1$) and hot ($x > 1$) plasmas. (j_{he} - hot electrons, j_{ce} - cold electrons, j_{hi} - hot ions, j_{he}^r - reflected hot electrons). $x < 1$: λ_{he} - units, $x > 1$: $10 r_D$ - units.
- Fig. 3: Schematic structure of the cold hot plasma interface (for descriptions of regions see Sec. 2.1)
- Fig. 4: Coordinate transformation, non-compensated current $-ej_e$ in the plasma shield and compensating current $-eI_0$ inside the structure. \mathbf{B}_0 guiding magnetic field, α - inclination angle, l thickness of the electric drift region.
- Fig. 5: Schematic current distribution in the toroidal geometry at inclined impact of hot plasma onto cold plasma shield.
- Fig. 6: Normalized energy deposition of hot electrons at perpendicular impact
- Fig. 7: Comparison of realistic y -component of magnetic field B_y outside of the shielding layer and that one used in the model.
- Fig. 8: $\mathbf{E} \times \mathbf{B}$ drift of the hot plasma and evolution of the shielding layer.
- Fig. 9: Piece-wise linear approximation of the effective potential φ in the magnetic pre-sheath ($x > L$) and the electrostatic sheath ($\varphi_L < \varphi < \varphi_0$ at $x = L$). x is given in the r_{hi} - units.
- Fig. 10: The dimensionless effective potential u and densities of electrons and ions in the electrostatic sheath at inclined impact. x is given in r_D - units.
- Fig. 11: The dimensionless effective potential u and plasma density n in the magnetic pre-sheath at inclined impact. x is given in r_{hi} - units.
- Fig. 12: Schematic distribution of effective (φ) and electric (ϕ) potential at inclined impact. Symbols $\Delta\varphi$ and $\Delta\phi$ show potential changes over the plasma shield. $x < L$: $\alpha\lambda_{he}$ - units.

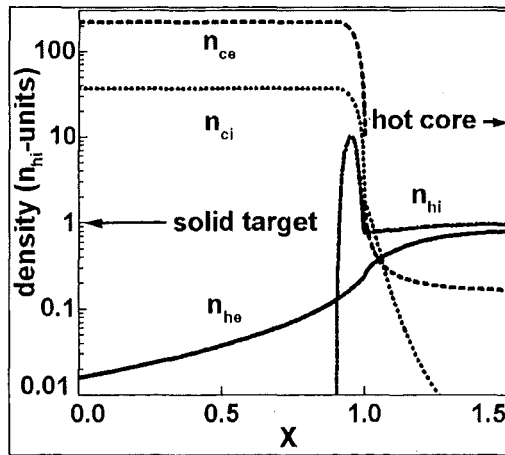


Fig.1: Density distribution of the cold and hot plasma ions (n_{ci} , n_{hi}) and electrons (n_{ce} , n_{he}). $x < 1$: λ_{he} - units, $x > 1$: $10 r_D$ - units.

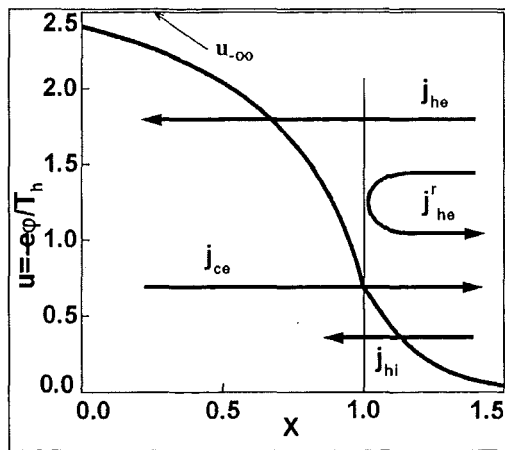


Fig.2: Dimensionless potential and particle fluxes in the cold ($x < 1$) and hot ($x > 1$) plasmas. (j_{he} - hot electrons, j_{hi} - hot ions, j_{he}^r - reflected hot electrons). $x < 1$: λ_{he} - units, $x > 1$: $10 r_D$ - units.

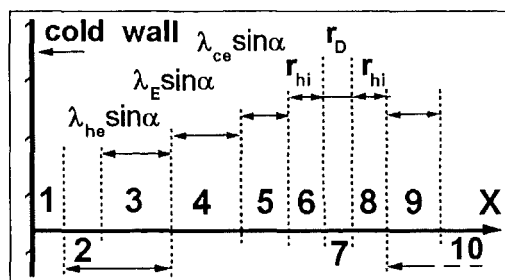


Fig.3: Schematic structure of the cold hot plasma interface.

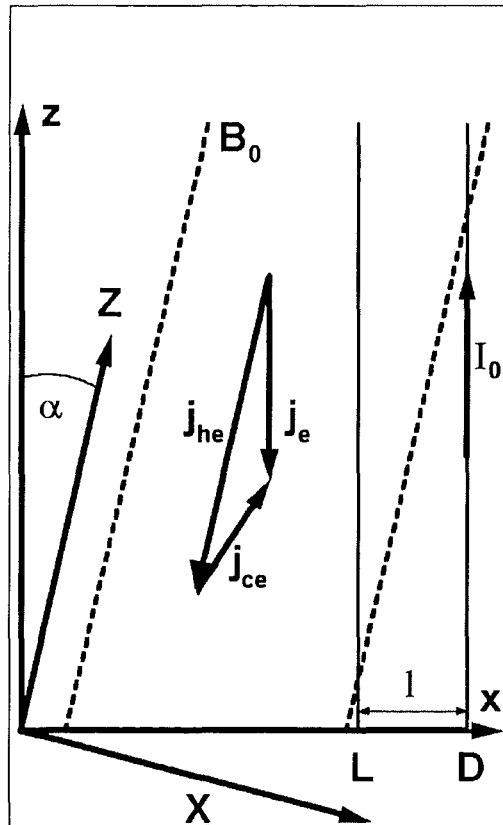


Fig.4: Coordinate transformation, non-compensated current $-ej_e$ in the plasma shield and compensating current $-eI_0$ inside the structure. B_0 guiding magnetic field, α inclination angle, l thickness of the electric drift region.

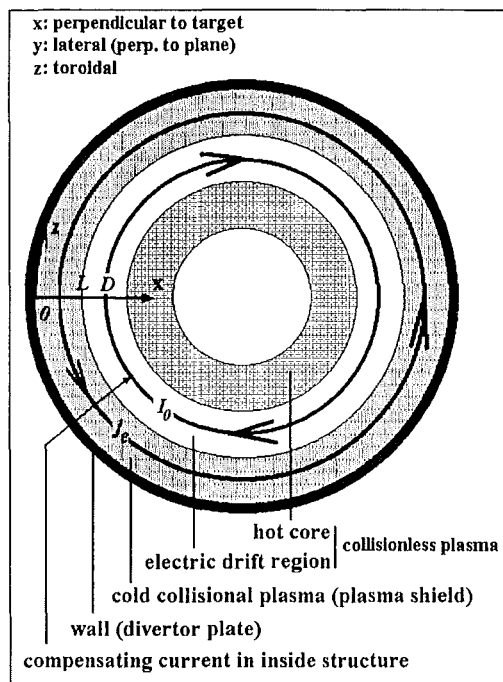


Fig.5: Schematic current distribution in the toroidal geometry at inclined impact of hot plasma onto cold plasma shield

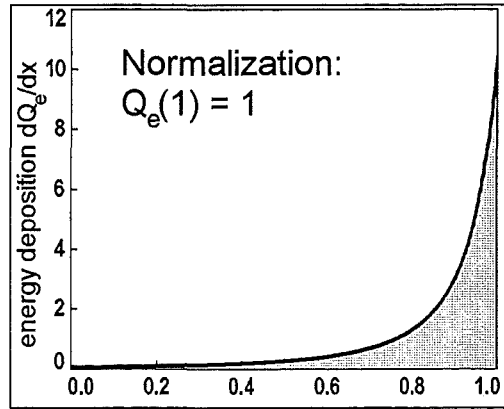


Fig.6: Normalized energy deposition of hot electrons at perpendicular impact. x is given in λ_{he} - units.

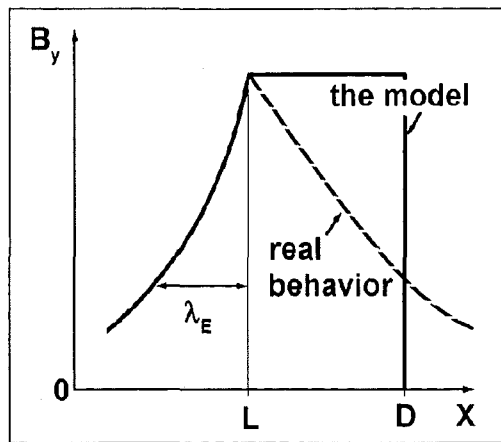


Fig.7. Comparison of realistic y -component of magnetic field B_y outside of the shielding layer and that one used in the model

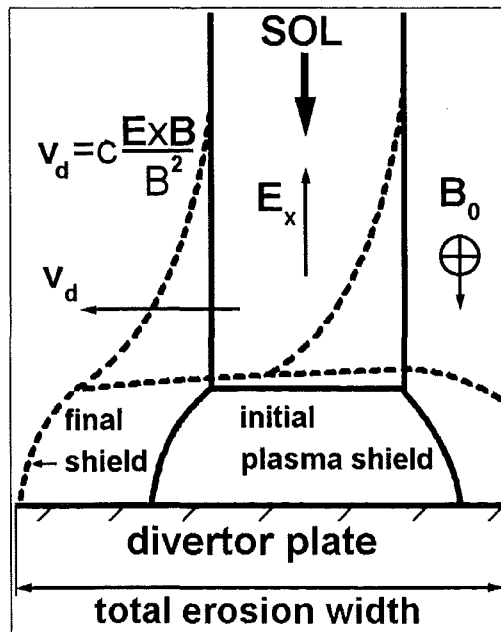


Fig.8: $E \times B$ drift of the hot plasma and evolution of the shielding layer.

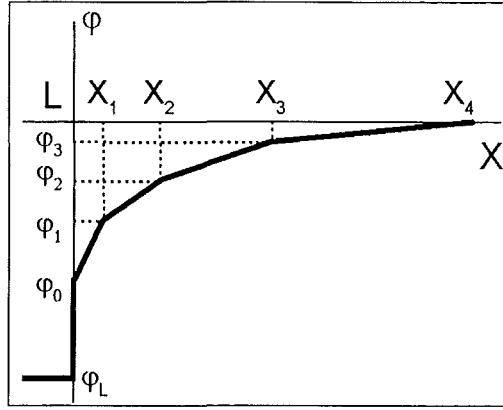


Fig.9: Piece-wise linear approximation of the effective potential ϕ in the magnetic pre-sheath ($x > L$) and the electrostatic sheath ($\phi_L < \phi < \phi_0$ at $x = L$). x is given in r_{hi} - units.

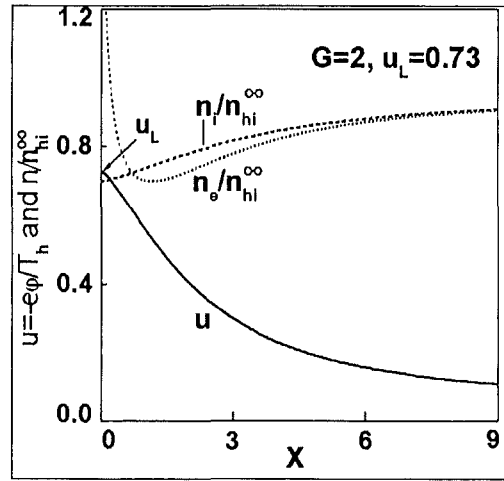


Fig.10: The dimensionless effective potential u and densities of electrons and ions in the electrostatic sheath at inclined impact. x is given in r_D - units.

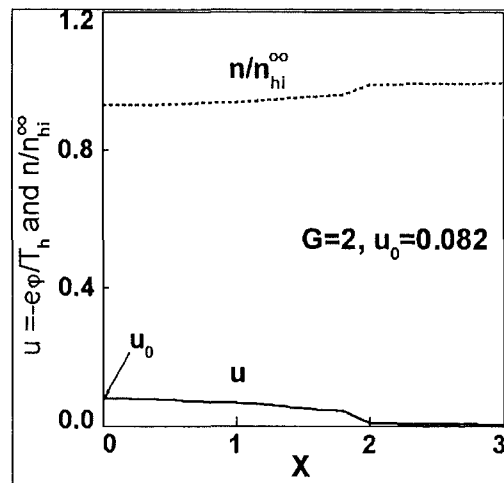


Fig.11: The dimensionless effective potential u and plasma density n in the magnetic pre-sheath at inclined impact. x is given in r_{hi} - units.

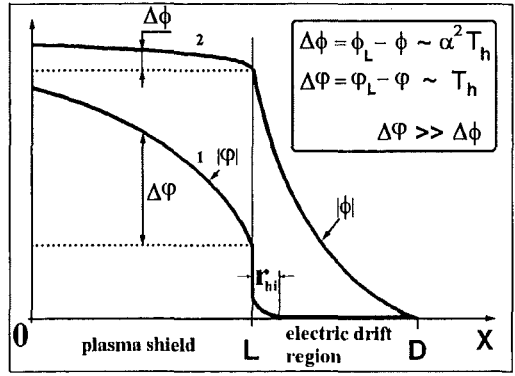


Fig.12: Schematic distribution of effective (ϕ) and electric (Φ) potential at inclined impact. Symbols $\Delta\phi$ and $\Delta\Phi$ show potential changes over the plasma shield. $x < L$: λ_{he} - units.